

Study of Reactive Sputtering Phenomena for Producing Oxide Thin Films

by

Israt Jahan



MASTER OF SCIENCE IN ELECTRICAL AND ELECTRONIC ENGINEERING

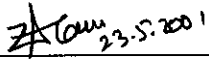
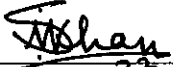


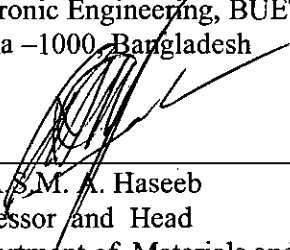
Department of Electrical and Electronic Engineering
BANGLADESH UNIVERSITY OF ENGINEERING AND TECHNOLOGY

May 2001



The thesis titled "Study Of Reactive Sputtering Phenomena For Producing Oxide Thin Films" submitted by Israt Jahan, Roll No.: 9506116F Session 1994-95-96 has been accepted as satisfactory in partial fulfillment of the requirement for the degree of MASTER OF SCIENCE IN ELECTRICAL AND ELECTRONIC ENGINEERING on May 23, 2001.

BOARD OF EXAMINERS

1.  23.5.2001
Dr. A.H.M. Zahirul Alam
Professor
Department of Electrical and
Electronic Engineering, BUET
Dhaka -1000, Bangladesh
Chairman
2.  23.5.2001
Dr. Shahidul Islam Khan
Professor and Head
Department of Electrical and
Electronic Engineering, BUET
Dhaka -1000, Bangladesh
**Member
(Ex-officio)**
3.  23.05.2001
Dr. Md. Shafiqul Islam
Associate Professor
Department of Electrical and
Electronic Engineering, BUET
Dhaka -1000, Bangladesh
Member
4.  23.5.2001
Dr. A.B.M. Harun-ur Rashid
Associate Professor
Department of Electrical and
Electronic Engineering, BUET
Dhaka -1000, Bangladesh
Member
5. 
Dr. A.S.M. A. Haseeb
Professor and Head
Department of Materials and
Metallurgical Engineering, BUET
Dhaka -1000, Bangladesh
**Member
(External)**

DECLARATION

It is hereby declared that thesis or any part of it has not been submitted elsewhere for the award of any degree or diploma.

Israt Jahan

.....
Israt Jahan

Contents

| | |
|---|-----------|
| List of Tables | iv |
| List of Figures | v |
| List of Symbols | vii |
| Acknowledgements | ix |
| Abstract | x |
| | |
| 1 Introduction | 1 |
| 1.1 Reactive Sputtering..... | 1 |
| 1.2 Background Historical Review of Research on Mechanisms in Reactive Sputtering | 3 |
| 1.3 Deficiencies in Current understanding..... | 11 |
| 1.4 Applications of Reactive Sputtering | 14 |
| 1.5 Objective..... | 14 |
| | |
| 2 Sputtering and Reactive Sputtering | 16 |
| 2.1 Sputtering..... | 16 |
| 2.2 Reactive Sputtering..... | 18 |
| 2.3 Hysteresis During Sputtering..... | 20 |
| | |
| 3 Process Modeling of Reactive Sputtering | 24 |
| 3.1 Introduction..... | 24 |
| 3.2 Modeling of Time –Dependent Change and Hysteresis..... | 27 |

| | | |
|----------|--|-----------|
| 3.2.1 | Theoretical Basis..... | 28 |
| 3.2.2 | Program. | 33 |
| 3.2.3 | Flow Chart | 35 |
| 4 | Discussions on Hysteresis Effects..... | 37 |
| 4.1 | Mass Balance Change During Compound Layer Formation and Sputter Etching..... | 37 |
| 4.2 | Mechanisms of Hystereis Formation..... | 38 |
| 4.3 | An Investigation of Hysteresis Effects as a Function of Pumping Speed and Sputtering Current..... | 40 |
| 4.3.1 | Effects of Pumping Speed..... | 40 |
| 4.3.2 | Effects of Sputtering Current..... | 46 |
| 5 | Conclusions | 51 |
| 5.1 | Conclusions..... | 51 |
| 5.2 | Recommendations for Further Work..... | 52 |
| | References..... | 53 |
| | Appendix | 56 |

List of Tables

- 1 Comparison between simulated and experimental results for increasing and decreasing reactive gas flow rate for different pumping speed.....45
- 2 Comparison between simulated and experimental results for increasing and decreasing reactive gas flow rate for different sputtering current.....50

List of Figures

| | | |
|------|--|----|
| 2.1 | Schematic representation of the plasma in planar diode sputtering | 17 |
| 2.2 | Schematic representation of reactive sputtering phenomena | 19 |
| 2.3 | Generic hysteresis curve for system pressure | 23 |
| 2.4 | Generic hysteresis curve for discharge voltage | 23 |
| 2.5 | Generic hysteresis curve for deposition rate | 23 |
| 3.1 | Schematic representation of particle fluxes during reactive sputtering | 24 |
| 3.2 | Schematic representation of reactive gas flow in reactive sputtering system | 28 |
| 4.1a | The variation of the sputtering rate for increasing and decreasing the reactive gas flow for a pumping speed of 0.2 m ³ /sec | 42 |
| 4.1b | The variation of the sputtering rate for increasing and decreasing the reactive gas flow for a pumping speed of 0.3 m ³ /sec | 42 |
| 4.1c | The variation of the sputtering rate for increasing and decreasing the reactive gas flow for a pumping speed of 0.4 m ³ /sec | 42 |
| 4.2a | The variation of reactive gas partial pressure for increasing and decreasing the reactive gas flow for a pumping speed of 0.2 m ³ /sec | 43 |
| 4.2b | The variation of reactive gas partial pressure for increasing and decreasing the reactive gas flow for a pumping speed of 0.3 m ³ /sec | 43 |
| 4.2c | The variation of reactive gas partial pressure for increasing and decreasing the reactive gas flow for a pumping speed of 0.4 m ³ /sec | 43 |
| 4.3a | The variation of oxide layer coverage at the target surface for increasing and decreasing the reactive gas flow for a pumping speed of 0.2 m ³ /sec | 44 |

| | | |
|------|--|----|
| 4.3b | The variation of oxide layer coverage at the target surface for increasing and decreasing the reactive gas flow for a pumping speed of 0.3 m ³ /sec | 44 |
| 4.3c | The variation of oxide layer coverage at the target surface for increasing and decreasing the reactive gas flow for a pumping speed of 0.4 m ³ /sec | 44 |
| 4.4a | The variation of sputtering rate for increasing and decreasing the reactive gas flow for a sputtering current of 1 Amp | 47 |
| 4.4b | The variation of sputtering rate for increasing and decreasing the reactive gas flow for a sputtering current of 2 Amp | 47 |
| 4.4c | The variation of sputtering rate for increasing and decreasing the reactive gas flow for a sputtering current of 3 Amp | 47 |
| 4.5a | The variation of reactive gas partial partial pressure for increasing and decreasing the reactive gas flow for a sputtering current of 1 Amp | 48 |
| 4.5b | The variation of reactive gas partial partial pressure for increasing and decreasing the reactive gas flow for a sputtering current of 2 Amp | 48 |
| 4.5c | The variation of reactive gas partial partial pressure for increasing and decreasing the reactive gas flow for a sputtering current of 3 Amp | 48 |
| 4.6a | The variation of oxide layer coverage at the target surface for increasing and decreasing the reactive gas flow for a sputtering current of 1 Amp | 49 |
| 4.6b | The variation of oxide layer coverage at the target surface for increasing and decreasing the reactive gas flow for a sputtering current of 2 Amp | 49 |
| 4.6c | The variation of oxide layer coverage at the target surface for increasing and decreasing the reactive gas flow for a sputtering current of 3 Amp | 49 |

List of Symbols

| | |
|-------------------|---|
| N | = Number of oxygen atoms reacted with metal atoms per unit area at the target surface . |
| F | = Flux of neutral reactive molecules onto a unit area at a partial pressure of P_N |
| J | = Current density of Ar ions |
| S_N | = Sputtering yield of the compound by incoming argon ions |
| α_t | = Sticking coefficient of the nitrogen molecule to the titanium target |
| α_c | = Sticking coefficient of the nitrogen molecule to the titanium covered part of the getter wall surface |
| Sg_0 | = Input gettering speed |
| St_0 | = Input target adsorbing speed |
| O_2 -flowmax | = Maximum O_2 flow rate in sccm |
| O_2 -flowint | = Minimum O_2 flow rate in sccm |
| O_2 -flowstep | = Step of O_2 flow rate in sccm |
| I-sp | = Sputtering current |
| Q_{in} | = The amount of introduced reactive gas |
| Site _t | = Number of sites on the gettering surface |
| Q_{ti} | = Number of incident positive ions |
| P | = Reactive gas partial pressure |
| Q_g | = The amount of gettered reactive gas |
| Q_t | = The amount of absorbed reactive gas |
| Sp | = Pumping speed |

Sp = Pumping speed
St = Target adsorbing speed
Sg = Gettering speed
Ym_m = Sputtering yield of metal
Ym_c = Sputtering yield of compound
Yg_c = Sputtering yield of compound
Flux_ar = Argon flux

Acknowledgements

The author wishes to express her profound gratitude and deep appreciation to her supervisor Dr. A.H.M.Zahirul Alam, Professor of the Department of Electrical and Electronic Engineering, BUET, for his affable guidance, constant supervision and continuous encouragement during the entire progress of the work. The author's ineffable indebtedness to him is indeed ineluctable for his valuable suggestions which greatly helped her in understanding the intricate problems involved in completing this work.

The author deeply remembers the loving support and inspiration of her family members in every step of the work.

ABSTRACT

Reactive sputtering is a technique to deposit compound thin films such as oxide, nitride, etc. It is well known that in reactive sputtering there are two operation modes: metal mode and compound mode. The transition between the two modes is generally avalanche-like and non-linear to reactive gas flow rate, and further shows hysteresis versus reactive gas flow rate. The nonlinear transition and hysteresis reduce controllability and reproducibility of the reactive sputtering process when it is operated in the near transition region. Therefore, it is thought to be crucial to reveal mechanisms involved in mode transition and hysteresis in order to improve stability and reproducibility of reactive sputtering.

In this thesis, the formation process of oxide films is investigated and discussed to reveal mechanisms of mode transition and hysteresis. Most importantly, effects of pumping speed and sputtering current on mode transition and hysteresis have been discussed. The simulation reveals that the origin of the hysteresis behavior is the difference of gettering capacity between metal mode and compound mode. Throughout the discussion, it is emphasized that reactive gas gettering plays an important role in the total mass balance changes in the reactive sputtering process.

On the basis of the discussion of the reactive sputtering process, a model simulating mode transition and hysteresis is presented. The model is based on the physical mechanism involved in target and wall behaviors. The important feature of the model is that hysteresis can be obtained as a result of the calculating of the time - dependent target condition changes. Hysteresis curves are obtained as a consequence of time-dependent calculations as a function of reactive gas mass flow rate. It is further shown by the simulation that the width of hysteresis strongly depends on pumping speed and sputtering current. These results satisfy the experimental results.



Chapter 1

INTRODUCTION

1.1 Reactive Sputtering

Initially, the term “sputtering” referred to the phenomena that target material was ejected as a result of the interaction between impinging ion and target atoms, and the subsequent interaction amongst the latter [1]. However, now-a-days especially in the field of thin film technologies, it refers to deposition of sputtered target materials onto substrate that locates typically on the opposite side of the target. The deposition process has currently been the main application of sputtering in the industrial fields. This process has the advantage in that it can deposit films with high adhesion to the substrates and with a high density without heating substrates. Furthermore, it is possible to obtain uniform coatings onto substrates with a large surface area by using planar magnetron method.

Recently, as demand for thin films has been increased, the importance of sputtering deposition has been greatly increased, especially in the fields of electronics, optics, and hard coatings. Progresses in vacuum apparatus including pressure gauges, gas flow control systems, etc., have also supported the application of this method for industrial purposes. Reactive sputtering is one technique involved in sputtering. In this process target that is nominally pure metal or alloy is sputtered in an atmosphere of reactive and inert gas mixtures. Sputtered target material reacts with reactive gas (e.g., O_2 , N_2 , etc.) on the substrate, resulting in the formation of compound films. A variety of compounds such as oxide, nitride, carbide, etc., have been deposited by this method. Today, application of reactive sputtering have been widened to the

fields of electronics, optics, hard coatings, decorative coatings, etc. The importance of reactive sputtering is rapidly increasing now a days.

In reactive sputtering it is known that there are two operation modes: metal mode and compound mode. In the metal mode, the target surface is kept metallic, and metallic films are deposited. On the other hand, in compound mode the target surface is covered by compound layers, and compound films are deposited. The condition of target covered by compound layers is sometimes referred as being "poisoned". The transition between these two operation modes is generally exhibited in the relation between total pressure or mass deposition rate and reactive gas flow rate. The transition is avalanche-like and nonlinear. The point where the mode transition occurs when the reactive gas flow rate is increased is different from the point where the transition occurs in the reverse direction when the reactive gas flow rate is decreased. This behavior is well known as a hysteresis behavior.

Since the mode transition and hysteresis affect the operating conditions strongly, understanding of their mechanisms is thought to be crucial to deposit films with good quality. Although many efforts have been made to understand the mechanisms of mode transition and hysteresis in reactive sputtering, these are still not well understood. The reason may be the complexity of phenomena involved in reactive sputtering. Therefore, a systematic study to reveal mechanisms involved in mode transition and hysteresis effects is indispensable to improve reactive sputtering process and widen its applications.

1.2 Background

Historical Review of Research on Mechanisms in Reactive Sputtering

In the early years of the research on reactive sputtering, only compound formation (oxidation, nitridation, etc.) on target surface attracted attentions because of its effects on the decrease in etching or sputtering rates.

The first report relating to the mechanisms of reactive sputtering was given by Greiner [2] on rf sputter etching in O₂. He assumed that the sputter and oxidation rates were independent and concurrent and indicated that the rate of change in target oxide thickness was given by:

$$dx/dt = R_{ox} - R_{sp}$$

Where R_{ox} is the oxidation rate and R_{sp} is the sputter rate of the target. At the equilibrium, dx/dt reaches 0 and no further changes occur in target oxide thickness.

In 1973, a report focusing on the mechanisms involved in reactive sputtering was given by Heller [3]. He reported a model for the reactive sputtering of metal in oxygen containing glow discharge. In the model, spontaneous oxide formation on the target surface and a sharp decrease in the sputtering rate were explained to occur at a definite oxygen partial pressure. The O₂ definite pressure was given as a function of the oxidation rate of the target relative to the sputtering rate.

In the middle 1970's, several authors reported target oxidation models and compared the results obtained by the proposed models with experimental results. Goranchev *et al.* proposed in 1976 a qualitative physical model explaining the influence of the oxygen content in the gas flow on the discharge current for reactive cathode sputtering in a dc diode system [4]. They

concluded that the increase in the oxygen content affected the discharge current density in two main ways: (i) by a sharp change in secondary ion-electron emission coefficient from the target surface as a result of its oxidation and (ii) by the influence of the oxygen content on the elementary ionization processes in the discharge region near the cathode as a result of the transition from a glow discharge in a noble gas to a glow discharge in oxygen. It was also shown that the experimental results with targets of different materials under different sputtering condition were in good agreement with the conclusion from the proposed physical model.

A model that explained deposition rate changes in reactive sputtering of metals in oxygen and nitrogen atmosphere in argon plasma was proposed by Abe and Yamashina, in 1976 [5]. The model is based on the difference between sputtering rate of the metal and its chemical compound, the surface coverage, the sticking probability, and incident flux of reactive gas atoms. The basic equation is:

$$dN/dt = \alpha(P/P_0)^n G(P)(1 - N/N_T) - B(N/N_T)$$

where P is the partial pressure of the reactive gas, P_0 is a constant related to the limiting pressure, N_T is the total number of active sites on the target surface that can be occupied by reactive gas atoms, N is the number of active sites that are occupied by reactive gas atoms under certain conditions, α is a constant, $\alpha(P/P_0)^n$ is the specific coefficient related to the sticking probability, B is the re-emission rate of reactive gas atoms when the target surface is completely covered with a monolayer of reactive gas atoms, $G(P)$ is the incident flux of reactive gas given by the kinetic theory of gases, and n is the order of the reaction. By giving the value of (α/B) , P_0 , and n , they calculated normalized sputtering rate for various systems such as Mo-O₂, Ti-O₂, and Ti-N₂. They also investigated Mo-O₂, Mo-N₂, Ti-O₂, and TiN₂ and found that there was an abrupt decrease in the sputtering rate in each experimental observation.

Donaghey et al. reported the effect of target oxidation on reactive sputtering rate of Ti in Ar-O₂ plasmas [6]. In their report it was concluded that the threshold of target oxidation was independent of the total plasma pressure and that it was specified uniquely by a critical mole fraction of oxidation in the plasma. They also reported that the sputter etch rate of the titanium target reached a maximum before the critical oxygen pressure and that the sputter deposition rate decreased sharply at a critical oxygen partial pressure. Furthermore, it was found that the time dependence of the target oxidation process was found to be in qualitative agreement with a target oxidation model.

In 1983, Maniv *et al.* reported that the oxidation was not so sensitive to whether a simple exponential,

$$(dx/dt)_{ox} = K \exp(-x/x_0)$$

or a parabolic,

$$(dx/dt)_{ox} = K_1/2x$$

rate was assumed [7]. They also reported that the oxygen flow rate at which an avalanche-like transition of the target surface condition occurred when O₂ flow rate was increased was different from that observed when O₂ flow rate was decreased after the target oxidation was completed. They further mentioned that, for O₂ flow rate less than the transition point, sputtered metal efficiently getters O₂. However, they did not discuss the origin of this behavior thoroughly. This behavior was later recognized as hysteresis effects in reactive sputtering.

As the existence of the abrupt transition of reactive sputtering process became recognized in late 1980's, some interests became to be taken in order to obtain a better process control in reactive sputtering processes. R. McMahon et al. first reported a control method by using constant cathode voltage control to obtain an AlN film with stoichiometry and reported mechanisms of the control [8,9]. In their reports, it was revealed that controlled cathode voltage at constant flow rates provided means for stable

operation for any degree of target coverage whereas controlled gas flow rates at constant power and controlled power at constant flow rates were found to exhibit runaway transitions associated with target coverage. They developed the model that allowed two distinct mechanisms of target coverage: chemisorption, and ion plating of reactive gas species to the target surface. By the model it was shown that, with the voltage control method, there was a one-to-one relationship between cathode voltage and film stoichiometry and that there was a method for calculating the film composition from the glow discharge characteristics alone.

In 1983 Reith *et al.* reported detailed results of the reactive sputtering of tantalum oxide for various target surfaces and O₂ flow rate conditions by observing partial pressure of O₂ during both reactive and non-reactive depositions [10]. They described the reactive sputtering of Ta in O₂ atmosphere in terms of two inverse reactions at two reactive surfaces: a dissociative reaction proceeded at the substrate. They concluded that a generalized process in which a metal oxide dissociated to a less-stable suboxide at the target, transferred to the substrate as the suboxide, and recombined to form the original target compound was applied for the reactive sputtering of any metal oxide that exhibited preferential sputtering effects.

In middle 1980's more efforts were performed to investigate reactive sputtering process, particularly hysteresis, quantitatively and to reveal mechanisms of hysteresis behavior. More attention was paid to the role of the gettering at the deposition area to reveal the correlation between target poisoning and gettering.

Hohnke *et al.* developed the model that described the reactive sputtering process in terms of three parameters: the reactive gas flow, the sputtering power, and the sputtering yield of the target [11]. The developed model established that the ratio of the sputtering power to the reactive gas flow rate was found to be as a fundamental parameter of reactive sputtering and

predicted accurately the magnitude of the ratio for the deposition of such diverse films as TiN and Cd₂SnO₄. Further, they first mentioned about the origin of the hysteresis behavior; the usual hysteresis effects mainly depended on intrinsic material properties, i.e., the difference in sputtering yield of the bare and nitrided or oxidized target surface and were weakly modified by varying process conditions. Although they gave a very clear explanation for the hysteresis behavior, their calculation was restricted only for the condition where stoichiometric films were deposited. In addition to this, they did not mention about effects of wall gettinger.

At almost the same time, Serikawa and Okamoto presented the effect of N₂ flow rate on Si rf reactive sputtering [12]. They investigated changes in the deposition rate, the sputtering pressure, and the nitrogen concentration in the film. Most important was that they first mentioned the effects of the pumping speed of the vacuum pump system on hysteresis behavior. It was shown that at a high Ar flow rate (high pumping speed) the hysteresis was distinguished. They also showed that the nitrogen partial pressure where the onset of the abrupt process change occurred increased as the sputtering power was increased or the pumping speed was increased. However, they did not consider a role of gettinger of reactive gas by sputtering metal.

Later they gave the explanation for the hysteresis formation by obtaining the relationship between the amount of consumed N₂ gas versus N₂ partial pressure [13]. Following their report, some authors mentioned that the hysteresis could be suppressed by increasing pumping speed of the vacuum pump system.

Until Serikawa and Okamoto first mentioned about consumption of reactive gas at chamber wall or substrate, no researcher had mentioned about the role of reactive gas consumption in mass balance changes in reactive sputtering.

Changes in sputtering yields during reactive sputtering have been also reported by several researches. Most of results have been examined in ion-beam sputtering. In 1980, Stein-bruchel *et al.* reported the results of sputtering yield measurements of metals and oxides of both Ti and Zr for neutrals and ions by collecting the sputtered species in a noble gas matrix and determining their amounts from optical adsorption spectroscopy [14]. They concluded that the atomic ion fractions for Ti and Zr bombarded by O_2^+ at 2keV are 0.8 and 0.4, respectively, whereas TiO and ZrO are sputtered largely as neutrals. They further reported that ratios of sputtering yields by bombarding 1keV O^+ ion to those by bombarding 1keV Ar^+ ion were about a half for Ti metal target and about one tenth for Zr metal target respectively.

In 1985, Gruen et al. examined effects of monolayer coverages on sputtering yield in ion beam sputtering by using laser fluorescence measurement [15]. In their report, it was revealed that Ti sputtering yield decreases as oxygen coverage on target surface was increased. The factor of decrease reported was 6 in the case of three- monolayer oxygen coverage compared to a clean Ti metal surface. Although the primary ion energy (about 3keV) used in their measurements ranged much higher than those of diode sputtering system, the reported results were useful to discuss effects of surface coverage change on sputtering yields in reactive sputtering.

In 1986, Betz and Husinsky also reported the results of investigation of sputtering yields changes under increased O_2 partial pressure conditions by using laser fluorescence spectroscopy and microbalance weight measurement method [16]. They summarized that sputtering yield decreased when 1×10^3 Pa of O_2 was introduced by a factor of about 5.1 for Cr, 1.8 for Ta, 2.7 for Ti, and 1.7 for Cu.

In 1984, Lemperiere et al. examined $Ti-N_2$ sputtering and reported that there was the abrupt decrease in deposition rate accompanied with film structure changes [17]. They also proposed a reactive sputtering model that

took into account the gettering effects of the deposited material. The model allowed the calculation of the determination of the deposition rate as a function of the reactive gas partial pressure. They obtained good agreement between experiment and theoretical values for the fractional surface coverage. This model is believed to be the first model that dealt with the gettering effects.

In relation with the hysteresis effects, Hmiel discussed the method to develop stable operation in the region where abrupt transition occurred in Ti-N₂ system [18]. He mentioned that there was a negative slope region of the equilibrium mass flow rate versus nitrogen partial pressure curve and that the existence of the negative slope was a phenomenon that could be observed with partial pressure control. It was also reported that the shape of the equilibrium flow versus partial pressure curve and the time response of the system were affected by the configuration of the sensor sampling port, the target, and the nitrogen gas inlet. He concluded that partial pressure control allowed access to pressure region that appeared to make superior TiN films, without hysteresis.

In 1987, Kadled et al. reported results of investigation of effects of pumping speed and cathode power in hysteresis in Ti-N₂ reactive sputtering [19]. In their experiments, total pressure was kept constant, so that if N₂ was consumed by gettering, Ar gas flow rates were increased. They assumed the existence of critical pumping speed to avoid hysteresis effects and gave the critical pumping speed from the calculation. In their calculation, they first gave the relation among masses of reactive gas introduced in the chamber, gettered, and pumped out and the relation between total pressure and N₂ partial pressure by the following equations:

$$\phi_r = p_r S_r + {}^s\phi_r$$

$$p_t = k_r p_r + k_i p_i$$

where ϕ_r is the mass of reactive gas introduced in the chamber, p_{rp} is reactive gas partial pressure, S_r is pumping speed for reactive gas, ${}^s\phi_r$ is reactive gas

gettered by deposited metal atoms, P_t is pressure, k_r is gauge sensitivity for reactive gas, k_i is gauge sensitivity for inert gas.

From the equations, the following equation was derived:

$$dp_r/d\phi = 1 / \{S_r + (d^s\phi/dp_r)\}$$

This equation meant that under the following conditions, the hysteresis effect could be avoided.

$$S_r + (d^s\phi_r/dp_r) < 0$$

Therefore, the critical pumping speed to avoid the hysteresis effect defined by the following equation:

$$S_c = (-d^s\phi/dp_r)_{\max}$$

From the experimental results, they concluded;

- i. The hysteresis effect can be avoided if the pumping speed is greater than the critical pumping speed.
- ii. Under the conditions that the ratio of N_2 flow rate and total pressure are constant, it is possible to avoid the hysteresis effect even if the pumping speed is smaller than the critical pumping speed.
- iii. Experimentally it was shown that the critical pumping speed does not depend on cathode power, substrate bias, and target-substrate distance although it is strongly depends on substrate temperature and total pressure; the critical pumping speed decreases with increasing substrate temperature and total pressure.
- iv. A smooth transition from the metal to the nitride mode in the relation between Ar flow rate and N_2 flow rate arises only in the absence of the hysteresis and at pumping speeds sufficiently higher than critical pumping speed.

More currently Berg et al. reported a model of hysteresis in a series of reports, by using a similar way to the model proposed by Abe and Yamashina

[20-21]. The proposed model can evaluate effects of process conditions such as pumping speed, sputtering power on hysteresis effects and predict the composition of sputtered materials as a result of calculation of transition curves. In their model they treated compound formation on the target surface and gettering at the deposition area by assuming coverage both for target and getter wall. By combining these two effects on target surface and on getter wall surface, they succeeded to show the abrupt transition in relationship between deposition rate and reactive gas (N_2) flow.

1.3 Deficiencies in Current Understanding

From reported experimental results to date, the following are generally recognized about mode transition and hysteresis in reactive sputtering:

- i. there is nonlinear behavior in relationship between deposition rate or reactive gas partial pressure after glow discharge ignition and reactive gas flow rate.
- ii. this non linear behavior is thought to be resulted from strong correlation between target poisoning or cleaning and reactive gas gettering on the chamber wall.
- iii. as a result of strong correlation, whole process condition drastically changes. This resultant process change is well known as an avalanche-like mode transition from metal to compound mode or from compound to metal mode.

- iv. the point where the mode transition occurs when reactive gas is increased is different from the point where the inverse mode transition occurs when reactive gas is decreased after the target poisoning is completed.
- v. the shape of hysteresis depends on pumping speed and cathode power or current.
- vi. higher pumping speeds reduce hysteresis width.
- vii. higher cathode power or current increases hysteresis width.

Although much knowledge has been accumulated especially in the last decade, there are still gaps in understanding of mechanisms of mode transition and hysteresis. In particular, mechanisms of mode transition and hysteresis have not been well understood, though they have been investigated by several authors. Furthermore, it is sometimes suggested that pumping speed affects mode transition and hysteresis and that there is a critical pumping speed at which hysteresis can be distinguished. However, no physical explanation has been given since effects of pumping speed on hysteresis has not been investigated for a range of pumping speed and sputtering current. Further, although gettering is believed to be a key to discuss mass balance changes in reactive sputtering, it has not been examined from the view point of qualitative relation to other paramount changes, as a function of reactive gas mass flow rate changes. Therefore, it is thought to be crucial to investigate gettering quantitatively. Effects of pumping speed and other parameters on mode transition and hysteresis should be investigated systematically to reveal mechanisms of mode transition and hysteresis.

Moreover, some models have been proposed on the basis of knowledge obtained empirically. However, since they are not based on physical mechanisms of target and wall phenomena, they cannot explain mechanisms of hysteresis and mode transition. Further, although time-dependent target

condition changes have been investigated and reported by several researchers, most of models deal with a steady – state condition, but no model has been reported that deals with time-dependent condition changes.

In addition, a model more currently proposed by Berg et al. explains hysteresis effects by obtaining an S-shape curve; i.e., they mentioned that hysteresis is formed as a result of a runaway process that occurred at a bend point of the S-shape curve [22-23]. However, the purpose of the modeling is to exhibit this runaway process by model calculation and explain mechanisms of avalanche-like process. In this respect, their model does not explain hysteresis effects that observed in an actual reactive sputtering process. They also mentioned that an S-shape curve was obtained in a system with a feed back system of reactive gas mass flow rate. However, the S-shape curve observed in an actual process is a consequence of the delay of the response time, and the shape of curve, therefore, mainly depends on a response time of the feed back system. Consequently, the approach used in Berg *et al.*'s model to explain hysteresis does not seem to be appropriate since an S-shape obtained in an actual process is not based on physical mechanisms of hysteresis behavior. Thus, it is also necessary to develop a model that involves physical mechanisms in mode transition and hysteresis. If the model is appropriate, it should exhibit time-dependent target condition changes and hysteresis without assuming how the process reaches a steady-state.

In conclusion, even though understanding of mechanism of reactive sputtering is a classical issue and there is much knowledge obtained both by experimental investigation and by modeling of the process, still there exist deficiencies in understanding of the process. Furthermore, a model that is based on the physical mechanisms involved in reactive sputtering and that deals with time-dependent target condition changes should be developed to examine mode transition and hysteresis effects.

1.4 Applications of Reactive Sputtering

The reactive sputtering process is a widely used technique for depositing compound films. By this technique oxides, nitrides, carbides and several other compounds are today routinely deposited in industrial plants.

Reactive sputtering process is used for manufacturing the following films:

- a) Super conductor films.
- b) Ferroelectric lead zirconate titanate(PZT, $\text{Pb}(\text{Zr},\text{Ti})\text{O}_3$) material are used for
 - DRAM
 - FRAM
- c) Storage tape devices
- d) Conducting films for
 - Flat panel
 - ITO display
 - Heating devices
- e) Nonconductive films

1.5 Objective

Reactive sputtering is a technique to deposit compound thin films such as oxide, nitride, etc. It is well known that in reactive sputtering there are two operation modes: metal mode and compound mode. The transition between the two modes is generally avalanche-like and non-linear to reactive gas flow rate, and further shows hysteresis versus reactive gas flow rate. The nonlinear transition and hysteresis reduce controllability and reproducibility of the reactive sputtering process when it is operated in the near transition region.

The objective of this study is to reveal mechanisms of mode transition and hysteresis behavior in reactive sputtering. In particular, effects of pumping

speed and sputtering current on mode transition and hysteresis will be discussed, since these parameters mainly affect reactive gas mass balance in the chamber. The model is based on the physical mechanism involved in target and wall behaviors. On the basis of the discussion of the reactive sputtering process, a model simulating mode transition and hysteresis is presented. The important feature of the model is that hysteresis can be obtained by the time-dependent changes in target condition. Hysteresis curves are obtained as a consequence of time-dependent calculations as a function of reactive gas mass flow rate. It is further shown by the simulation that the width of hysteresis strongly depends on pumping speed and sputtering current.

Chapter 2

SPUTTERING AND REACTIVE SPUTTERING

2.1 Sputtering

Sputtering is a process whereby material is dislodged and ejected from the surface of a solid or a liquid due to momentum exchange associated with surface bombardment. A surface of coating material called target is placed into a vacuum chamber along with the substrates and the chamber is evacuated to a pressure range of 5×10^{-4} to 5×10^{-7} Torr. The bombarding species are generally ions of a heavy inert gas. Argon is most commonly used. The substrates are positioned in front of target so that they intercept the flux of sputtered atoms.

The most common method of providing the ion bombardment is to backfill the evacuated chamber with the inert gas to pressure from 1 to 100 m Torr and ignite an electric discharge so that ionization of the working gas occurs in the region adjacent to the target (Fig. 2.1). Such a low pressure electric discharge is called a glow discharge, and the ionized gas is called plasma. The target is negatively biased so that its surface is bombarded by positive ions from the plasma. The most direct method for providing the plasma, the target ion bombardment, is simply to make the target the cathode, or negative electrode, or the electric discharge. Applied potential between the target and the anode are typically from 500 to 5000 V. A sputtering apparatus with this design is called a diode. The glow discharge in such a device is of a form called an abnormal negative glow.

The most striking characteristic of the sputtering process is its universality. Since the coating material is passed into the vapor phase by mechanical (momentum exchange) rather chemical or thermal process, virtually any material is a candidate coating. DC methods are generally used for sputtering

metals. An rf potential must be applied to the target in order to sputter nonconducting materials.

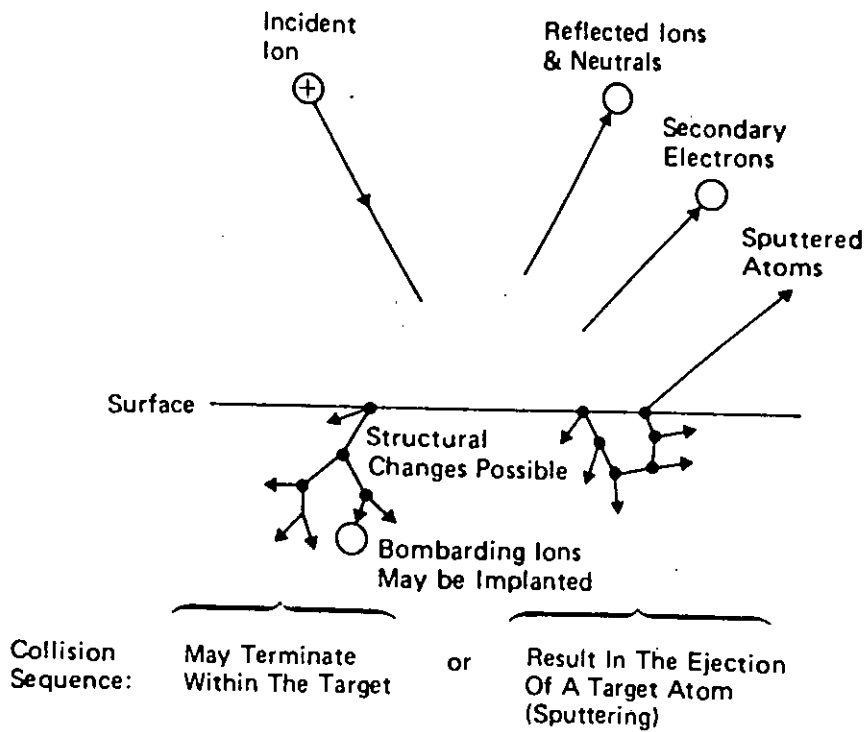


Fig. 2.1 Schematic representation of the plasma in planar diode sputtering

Sputter coating technology includes many variations of the basic process described above. For example, coating may be formed by-

- i. Employing a target, which is a mosaic material.

- ii. Employing several targets simultaneously, of identical or different materials.
- iii. Employing several targets sequentially to create a layered coating.
- iv. Biasing the substrate as an electrode prior to coating, so that contamination is removed by sputtering, and coating nucleation sites are generated on the surface. This is known as sputter cleaning.
- v. Biasing the substrates as an electrode to cause surface ion bombardment during deposition, in order to remove loosely bonded contamination or to modify the structure of resulting coating. This is known as bias sputtering.
- vi. Employing a gas to introduce one of the elements of coating materials into the chamber. This process is known as reactive sputtering. It permits metal targets and dc power supplies to be used in preparing coatings of nonconducting compounds.

2.2 Reactive Sputtering

Reactive sputtering is one technique involved in sputtering. In one form of reactive sputtering, the target is nominally pure metal, alloy, or mixture of species, which one desires to synthesize into a compound by sputtering in a pure reactive gas or an inert gas reactive gas mixture. The reactive gas either is, or contains the ingredient required to synthesize the desired compound. The second type of reactive sputtering involves a compound target that chemically decomposes substantially during inert gas ion bombardment, resulting in a film deficient in one or more constituents of the target. In this case, a reactive gas is added to make up for the lost constituent.

The main difference between these two types of reactive sputtering has to do with the deposition rate dependence on partial pressure of the reactive gas. A large number of reactive gases have been used to synthesize compounds from metal targets or to maintain stoichiometry in the face of decomposition: Air O_2 or H_2O (oxides), N_2 or NH_3 (nitrides), O_2+N_2 (oxy-nitrides), H_2S (sulfides), C_2H_2 or CH_4 (carbides), SiH_4 (silicates), HF or CF_4 (fluorides), As (arsenides). etc. These are obvious safety problems with some of these gases.

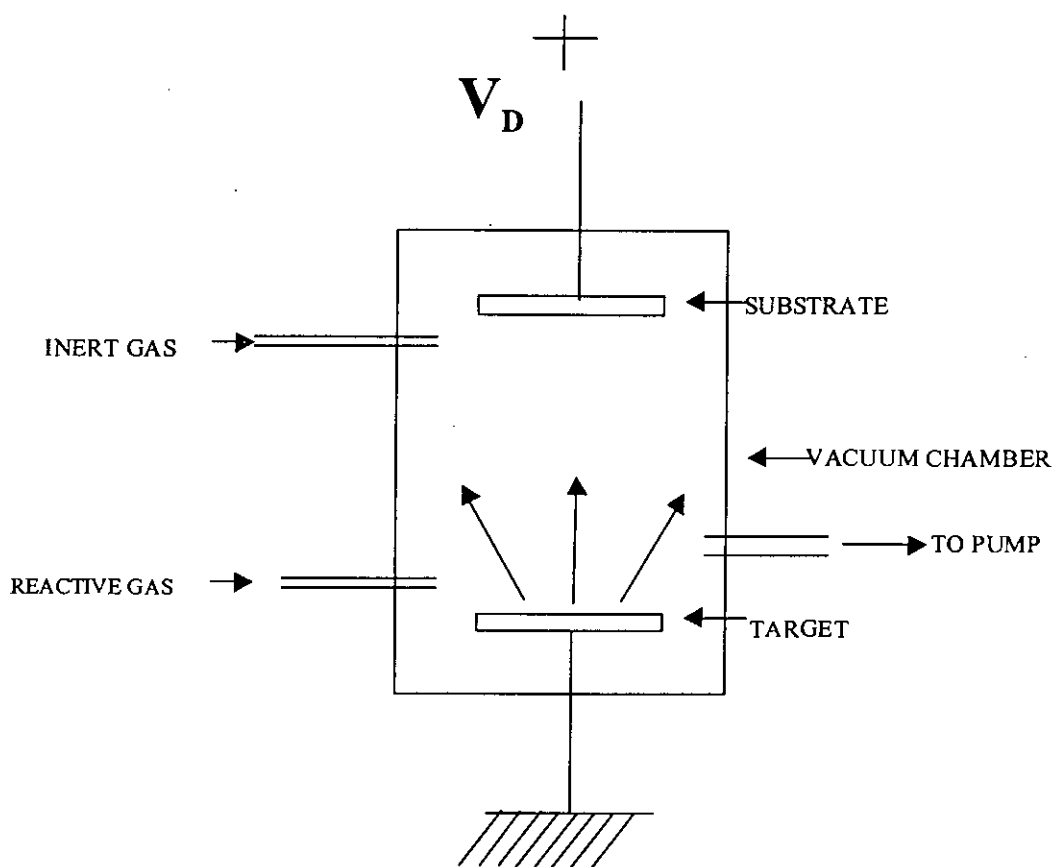


Fig. 2.2 Schematic representation of reactive sputtering phenomena.

The advantages of this technology using metal target are

- Metal target can be machined;

- Metal targets have high thermal conductivity and, therefore, can handle high power densities without cracking;
- Different types of compounds can be fabricated by choosing different reactive gas mixtures; and
- High rate techniques give deposition rates comparable to those of pure metals.

2.3 Hysteresis During Sputtering

The two regimes can be conveniently discriminated by reference to the hysteresis curve of total system pressure during sputtering, p (in Pa or Torr) as a function of the flow rate f_r of the reactive gas into the system. A generic hysteresis curve is shown in Fig. 2.3; it would apply for example, to the sputtering of In in an Ar/O₂ mixture. A constant pressure, P_a is maintained by the flow f_a (in sccm) of non reactive gas (e.g., Ar) into the continuously pumped system, P_a is the Ar pressure at which the In target would be sputtered to deposit an In film. The dashed line in Fig. 2.3 shows the linear increase in p that would result from increasing f_a ; this follows from the relation $Q=Sp$, where Q is the total flow rate of gas and S is the pumping speed.

When f_r is increased, however, the total pressure does not increase in this way because the gas reacts with the metal; e.g., In₂O₃ is formed by the reaction of O₂ with In. As shown by the solid line in Fig. 2.3, p remains essentially constant at the initial value, p_a , until a flow rate f_1 , when it increases to a new value, p_1 . If no sputtering took place, the value of p at this total flow rate would be p_0 : $\Delta p = p_0 - p_1$ is the reduction in pressure due to the reactive sputtering. Once the equilibrium value of p has been established, subsequent changes in f_r cause p to increase or decrease linearly: at each value of f_r , the difference Δp between the system pressure with and without

reactive sputtering is constant. However, if f_r is reduced to value f_{r2} , Δp increases and the system pressure decrease from p_2 to the initial value, p_a

The hysteresis curve represents two stable states of the system with rapid transition between these two states. In state A, there is negligible change in the total pressure as f_r is varied; in state B, the pressure varies linearly with f_r but is lower by Δp than the total pressure measured in the absence of sputtering. In state A essentially all the reactive gas is being used in the deposition of film and the atomic ratio, y , of the reactive gas to sputtered metal in the film increases with f_r . Thus, state A can be considered as a regime in which the sputtered metal is doped with reactive gas. In state B, a constant volume of reactive gas is consumed, independent of f_r , and there is an excess of reactive gas so that the formation of a stable compound is favored. The rate at which the reactive gas is consumed in the sputtering process is, therefore,

$$Q_a = f_r \quad \text{and}$$

$$Q_b = (f_{r1} - f_{r2}) \cdot (p_0 - p_1) / (p_1 - p_2)$$

in state A and B respectively. State A is known as metallic mode and state B is known as oxide mode. The transition from state A to B is due to the formation of a compound on the surface of the metal sputtering target.

The voltage and deposition rate hysteresis are also shown in Figs. 2.4 and 2.5. The voltage decrease at high oxygen injection rate corresponds is the metal-to-compound transition. The voltage increase at low injection rates represents the compound-to-metal transition. The reduction of deposition rates believed to result primarily from compound formation on the cathode surface and from the reduced sputtering yield of the reactive gas molecules. The compounds often have higher electron secondary emission coefficients, which results in a reduction in both the discharge voltage and the ion component in the cathode current, for discharges driven at constant currents.

A cathode on which compound layer has formed is often referred as being "poisoned". The effect of poisoning on the reactive sputtering process depends on the metal-reactive gas combination and the properties of the cathode surface layers.

The poisoning effects introduce to practical problems. One is the loss in deposition rates. The second is that during the transition the material being deposited often passes abruptly from a metal to a nearly full-stoichiometry compound. Intermediate materials, such as suboxides therefore become difficult to deposit. Consequently, considerable work has been directed toward trying to operate sputtering sources right at or very near the transition point, with, in most cases, not much success.

It is important to realize that the reactive sputtering process is dependent on the total system; i.e., its geometry, the accumulation of coating on walls and fixtures, and the positions of gas injection. All these parameters must be carefully controlled in order for reactive sputtering to be effectively used on a production basis.

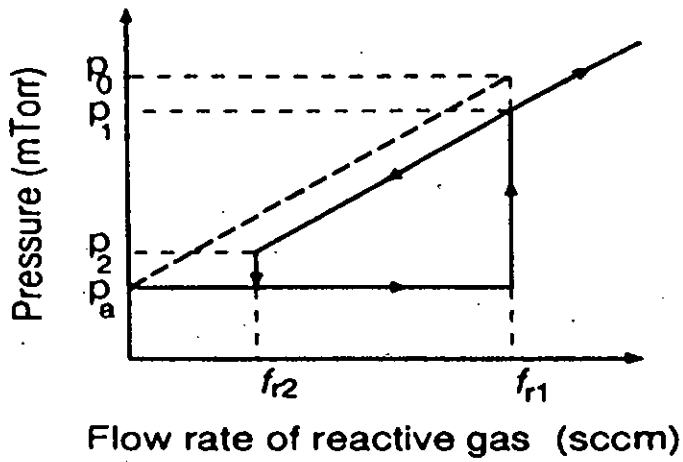


Fig. 2.3 Generic hysteresis curve for system pressure.

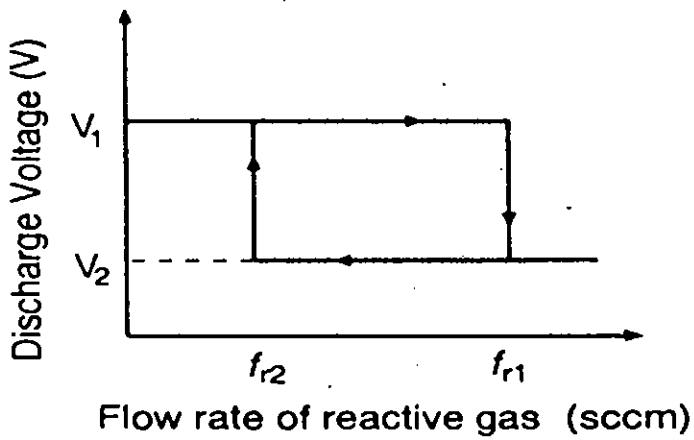


Fig. 2.4 Generic hysteresis curve for discharge voltage.

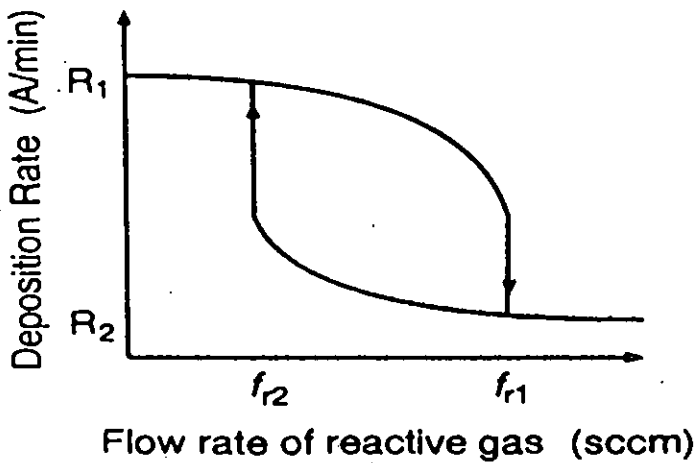


Fig. 2.5 Generic hysteresis curve for deposition rate.

Chapter 3

PROCESS MODELING OF SPUTTERING

3.1 Introduction

Modeling is sometimes useful to examine process conditions. There have been some models to examine reactive gas mass balance in reactive sputtering processes. More currently, Berg et al. [23,24] reported a model of hysteresis. In his model he treated compound formation on the target surface and gettering at the deposition area by assuming coverage both for target and getter wall (Fig. 3.1).

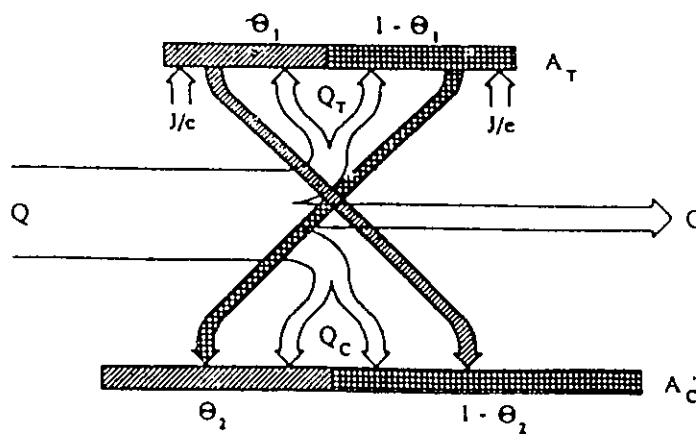


Fig. 3.1 Schematic representation of particle fluxes during reactive sputtering

The basic equations in their model are the mass balance equation between the reaction and sputter removal at the target and that between deposited metal atoms and adsorbing reactive gas atoms at getter wall surface during deposition; the former one is as follows:

$$dN/dt = 2\alpha_t F(1-\theta_1) - (J/e)S_N\theta_1 \dots \dots \dots (3.1.1)$$

where, N is the number of reactive gas atoms reacted with metal atoms per unit area at the target surface,

F is the flux of neutral reactive molecules onto a unit area at a partial pressure of P_N ,

J is the current density of Ar ions causing sputtering from the target surface by reactively formed compound ,

S_N is the sputtering yield of the compound by the incoming argon ,and

α_t is the sticking coefficient of the reactive gas molecule to the metal target.

The mass balance equation at the getter wall surface is given by:

$$dN/dt = 2\alpha_c F(1-\theta_2) + (J/e)S_N\theta_1(A_t/A_c)(1-\theta_2) - (J/e)S_M(1-\theta_1)(A_t/A_c)\theta_2 \dots \dots \dots (3.1.2)$$

Where, S_M is sputtering yield of the elemental metal by incoming argon ions,

θ_2 is relative coverage of the getter wall surface of the reactively formed compound ,and

α_c is the sticking coefficient for the nitrogen molecules to the metal covered part $(1-\theta_2)$ of the getter wall surface.

The first term $2\alpha_c F(1-\theta_2)$ in the equation denotes the spontaneous reaction by neutral reactive molecules of the free metal molecule at the getter wall surface.

The coefficient, $(J/e)S_N \theta_1$, in the second term in the equation is the sputtering rate of compound from the target. They assumed that all the material sputtered from the target area A_t will arrive at the getter wall surface. This area is denoted A_c . Thus, the deposition rate of sputtered compound portion from the target that arrives to the getter wall A_c will be $(J/e)S_N \theta_1 (A_t/A_c)$ due to the difference in the area of the target and the getter wall surface. A fraction $(1-\theta_2)$ will be deposited onto non-reacted metal on the getter surface. Thus, the change in population of the compound portion on the surface increases with the amount given by:

$$(J/e)S_N \theta_1 (A_t/A_c)$$

The factor $(J/e)S_M(1-\theta_1)$ denotes the sputtering of elemental metal from the target. In the same way, the deposition rate onto the getter wall surface will be then given by:

$$(J/e)S_M (1-\theta_1)(A_t/A_c) \theta_2$$

The part of sputtered metal that is deposited onto the $(1-\theta_2)$ covered fraction of the getter wall will not change the population of nitride on the getter wall.

Under the steady conditions, $dN/dt=0$ for both target surface and getter wall surfaces, from Eq. (3.1.1), the relationship is given by:

$$2\alpha_t F(1-\theta_1) - (J/e)S_N \theta_1 = 0 \dots \dots \dots (3.1.3)$$

and from Eq.(3.1.1).

$$2\alpha_c F(1-\theta_2) + (J/e)S_N \theta_1 (A_t/A_c)(1-\theta_2) - (J/e)S_M(1-\theta_1)(A_t/A_c)\theta_2 = 0 \dots \dots \dots (3.1.4)$$

They obtained consumption of reactive gas in the process chamber:

$$Q_t = \alpha_t F(1-\theta_1) A_t \dots \dots \dots (3.1.5)$$

$$Q_c = \alpha_c F(1-\theta_2) A_c \dots \dots \dots (3.1.6)$$

The flux intensity of neutral reactive gas can be calculated from the kinetic theory:

$$F = P_N / (2\pi kTM)^{1/2} \dots\dots\dots (3.1.7)$$

where M is the mass of the reactive gas molecule. The total sputtering rate can be obtained by

$$R = (J/e)(S_N\theta_1 + S_M(1-\theta_2)) \dots\dots\dots (3.1.8)$$

From these equations systems, they can find analytical expression for θ_1 , θ_2 , P_{N2} , and R as a function of incoming reactive gas mass flow q_p .

However, the developed model does not consider elapsed time for process modeling.

3.2 Modeling of Time-Dependent Process Change and Hysteresis

In this chapter, a model of reactive sputtering that calculated target compound-layer formation and sputter-etching as a function of elapsed time will be proposed. The model will provide hysteresis curves as a result of the calculations of target coverage changes (compound-layer formation and sputter-etching) as a function of reactive gas mass flow rate. The simulation will be performed by dealing with mass balance among the amount of gas gettered at the chamber wall, the amount of gas adsorbed at the target surface, the amount of gas sputtered from the target surface, and the amount of gas pumped out. It will be emphasized that modeling of reactive sputtering should involve simulation of compound-layer formation and sputter-etching as a function of elapsed time since nonlinear behavior and hysteresis in reactive sputtering are principally resulted from the balance between compound –layer formation and sputter-etching.

3.2.1 Theoretical Basis

The fundamental idea for modeling is given by considering reactive gas flow in reactive sputtering process. Flow of reactive gas is schematically shown in Fig.3.2. Introduced gas molecules react with active metal atoms at the target surface and from compound layers, and are gettered at the wall surface by sputtered metal flux. Simultaneously they are pumped out by the vacuum pump. Gas adsorbed on the target surface is sputtered as well as the metal target material is. Deposition of the gas gettered at the chamber at the chamber wall is usually negligible. This relationship is given by:

$$Q_{in} = Q_a - Q_s + Q_g + Q_p \dots \dots \dots (3.2.1.1)$$

Where, Q_{in} is the amount of introduced reactive gas,

Q_a is the amount of reactive gas adsorbed at the target,

Q_s is the amount of reactive gas sputter from the target,

Q_g is the amount of reactive gas gettered at the chamber wall, and

Q_p is the amount of reactive gas pumped out.

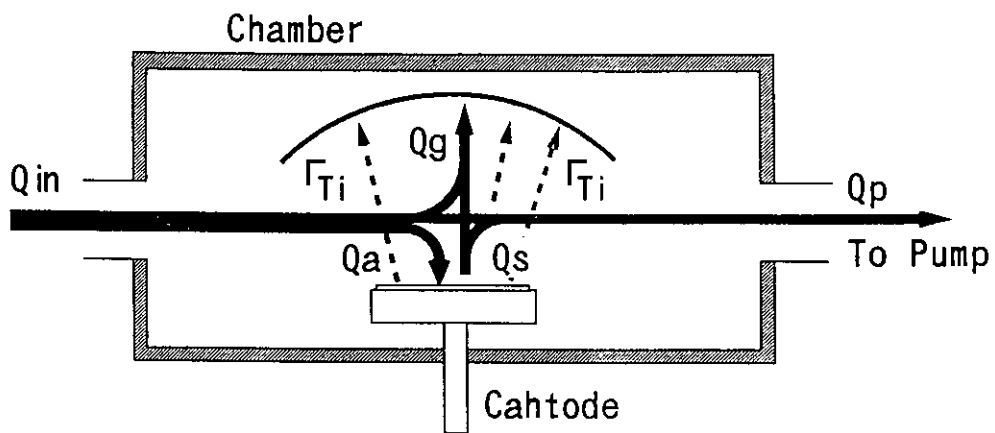


Fig. 3.2 Schematic representation of reactive gas flow in reactive sputtering system

This equation (3.2.1.1) can also be expressed by the following equation:

$$Q_n + Q_s = P(S_a + S_g + S_p) \dots \dots \dots (3.3.1.2)$$

Where, P is reactive gas partial pressure,

S_a is target adsorbing speed,

S_g is gettering speed, and

S_p is pumping speed of the vacuum pump system.

Then, reactive gas partial pressure P can be given by:

$$P = (Q_{in} + Q_s) / (S_a + S_g + S_p) \dots \dots \dots (3.2.1.3)$$

This equation must be satisfied during moment-by-moment mass balance changes. S_p and Q_{in} are treated as constant values within the pressure range to be considered. Other terms depend on elapsed time i.e., P, Q_s, S_a, and S_g change as a function of elapsed time until the process reaches a steady-state.

There may be some approaches to display the change in P as a function of elapsed time. To understand and simulate mechanisms of reactive sputtering it is better to express Q_a, S_a, and S_g as a function of target coverage θ as a function of elapsed time. As shown below, this is possible by treatment of Q_s, S_a, and S_g.

Adsorption of reactive gas at the target surface is shown as a function of target coverage by the following equation:

$$Q_a = \Gamma_{O_2} \alpha_T (1 - \theta) A_T \dots \dots \dots (3.2.1.4)$$

Where Γ_{O₂} is O₂ flux, α_T is adsorption coefficient at the target wall, and A_T is target surface area.

By introducing reactive gas partial pressure P, Eq.(3.2.1.4) can be written by:

$$Q_a = PC_1 \alpha_T (1 - \theta) A_T \dots \dots \dots (3.2.1.5)$$

Where C_1 is a constant.

Since $S_a = Q_a/P$, the following equation is obtained:

$$S_a = C_1 \alpha_T (1-\theta) A_T \dots\dots\dots (3.2.1.6)$$

By this equation, S_a can be expressed as function of θ by determining C_1 , α_T , and A_T . A constant C_1 can be given from a kinetic theory, whereas α_T and A_T in an actual situation vary as a function of P and θ . Although theoretically it is possible to provide α with a change in P , this makes the model much more complicated and actually makes it disable to solve. In other words, it is very difficult to give an accurate value for α in a moment-by-moment model calculation. In addition, it is also thought to be meaningless to use a value of an appeared surface area as A_T .

As a consequence of this discussion, a constant that is equal to $C_1 \alpha_T A_T$ is introduced. This covers the problem described above, and further simplifies the calculations. Thus Eq.(3.2.1.6) can be written as the following equation:

$$S_a = C_1' (1-\theta) \dots\dots\dots (3.2.1.7)$$

In the computer program, C_1' is given as an initial target adsorption speed, S_t^0 .

The gettering at the chamber wall surface can be also provided as a function of θ . The gettering amount is determined from the amount of incident reactive gas and the number of metal sites that can adsorb reactive gas atoms or molecules. The relationship will be given by the following equation:

$$Q_g = \Gamma_0 \alpha_w Q_m A_w / N_s \dots\dots\dots (3.2.1.8)$$

Where α_w is adsorption coefficient of reactive gas at chamber wall, Q_m is the number of active metal sites at the chamber wall, A_w is the area of the gettering

surface, and N_s is the number of sites on the gettering surface. By introducing P, Eq.(3.2.1.8) can be rewritten by the following equation:

$$Q_g = PC_2 \alpha_w Q_m A_w / N_s \dots \dots \dots (3.2.1.9)$$

By the same way used in the case of dealing with target behavior, S_g is given by:

$$S_g = C_2 \alpha_w Q_m A_w / N_s \dots \dots \dots (3.2.1.10)$$

Since active metal atoms that can adsorb reactive gas are provided by sputtering, the number of active metal site, Q_m is given by the following equation:

$$Q_m = Q_i (Y_c \theta + Y_m (1 - \theta)) \dots \dots \dots (3.2.1.11)$$

Where Q_i is the number of incident positive ions (e.g., Ar^+) on the whole target area, Y_c is sputtering yield for the compound-covered surface of the target and Y_m is sputtering yield for the metallic surface of the target. In this treatment the wall surface area is not considered; i.e., it is assumed that sputtered metal atoms can adsorb reactive gas anywhere the metal atoms deposit. In addition, it is assumed that the metal atoms covered with newly arriving metal atoms cannot adsorb reactive gas atoms.

From Eqs.(3.2.1.10) and (3.2.1.11), the following equation is obtained:

$$S_g = C_2 \alpha_w Q_i (Y_c \theta + Y_m (1 - \theta)) A_w / N_s \dots \dots \dots (3.2.1.12)$$

By a similar approach to dealing with target behavior, the equation is simplified as follows:

$$S_g = C_2' (Y_c \theta + Y_m (1 - \theta)) \dots \dots \dots (3.2.1.13)$$

Thus, S_g is determined by Q_i , Y_c , Y_m , and θ . In the computer program C_2' is given as an initial gettering speed, S_g^0 .

The remaining term, Q_s , is given by the following equation

$$Q_s = Q_i Y_c \theta \dots \dots \dots (3.2.1.14)$$

For this equation, Q_i is determined from sputtering current.

As a consequence, P can be expressed as a function of θ :

$$P=(Q_{in}+QY_c\theta)/(C_1(1-\theta)+(C_2Q_i(Y_c\theta+Y_m(1-\theta))+S_p))\dots\dots\dots(3.2.1.15)$$

The change in θ is given as a function of elapsed time from the result of the calculation of the amount of reactive gas adsorbed on the target surface and sputtering off from the target. The equations to calculate these amounts are derived from Eqs. 11 and 14.

There are two ways to obtain changes in P and θ as a function of elapsed time; one is to include the differentiation of Eq.(3.2.1.15) for elapsed time, and the other is a time-incremental method. The differentiation seems to require considerably complicated equations to solve. Compared to the differentiation, the time-incremental method is simpler and easier since it is unnecessary to use a complicated differentiation, i. e., since elapsed time is used as a calculation step of the simulation program, it is unnecessary to use the differentiation. Thus the time-incremental method is thought to be better for the purpose of modeling, and preferred as the method to solve the problem. Furthermore, in this method, since a computer is used as it was an actual process chamber, it become easier for us to understand what obtained results mean. The use of the time-incremental method is a feature of this simulation.

3.2.2 Program

In the program, Ti-O₂ reactive sputtering is modeled. First the constants are given: S_g^0 , S_t^0 , N_s , Y_m , and Y_c . Typical values of the constants are: $S_g^0=3.0 \times 10^{-1} \text{ m}^3/\text{s}$, $S_t^0=20 \text{ m}^3/\text{s}$, $N_s=10^{18}$, $Y_m=2.3 \times 10^{-1}$, and $Y_c=1.5 \times 10^{-2}$. For calculation of target compound-layer formation the initial θ is given as 0, whereas for that of target sputter-etching it is given as unity.

Then the calculation is progressed with an increase of time increment. At time step, $T=t$, first, reactive gas partial pressure P is calculated from Q_{in} , S_p , S_t at $T=t-1$, and S_g at $T=t-1$:

$$P(t)=Q_{in}/(S_p+S_t(t-1)+S_g(t-1)) \dots \dots \dots (3.2.2.1)$$

Then $Q_i(t)$ and $Q_g(t)$ are calculated:

$$Q_i(t)=P(t)S_t(t-1) \dots \dots \dots (3.2.2.2)$$

$$Q_g(t)=P(t)S_g(t-1) \dots \dots \dots (3.2.2.3)$$

Then target coverage $\theta(t)$ is calculated:

$$\theta(t)=\theta(t-1)+Q_i(t)/((1-\theta(t-1))N_s) \dots \dots \dots (3.2.2.4)$$

If calculated $\theta(t)$ exceeds 1, $Q_i(t)$ is recalculated from the number of target surface sites so that θ becomes unity. In this case, $P(t)$ is also recalculated from the newly determined $Q_i(t)$ to satisfy Eq.(3.2.1.15).

If there are no sufficient numbers of wall sites to getter reactive gas, an excess amount of reactive gas is added to the amount of introduced gas at the next step, $T=T+1$.

Next, sputtering of target is dealt with. The amount of sputtered Ti is given by the following equation:

$$Q_m(t)=((1-\theta(t))Y_m+\theta(t)Y_c)Q_i \dots \dots \dots (3.2.2.5)$$

Here, N_s is not considered since Q_i is smaller than N_s in the program. The amount of Q_m determines the capacity of the gettering pump at $T=t+1$. Then a part of O_2 is gettered if there are active metal sites on the wall to getter sputtered gas. Not-gettered gas is also treated as an additional over flow. A new value of $\theta(t)$, $\theta'(t)$, is calculated from the following equation:

$$\theta'(t) = \theta(t) - \theta(t) Y_c Q_i / N_s \dots \dots \dots (3.2.2.6)$$

Then the amount of sputtered reactive gas is calculated from the change in θ :

$$Q_s(t) = (\theta(t) - \theta'(t)) N_s \dots \dots \dots (3.2.2.7)$$

Then if there is enough numbers of active metal site on the wall to getter sputtered gas, sputtered gas is gettered. Not-gettered gas is also treated as another over flow.

Finally, new pumping speeds, $S_t(t)$ and $S_g(t)$ are calculated from $\theta'(t)$:

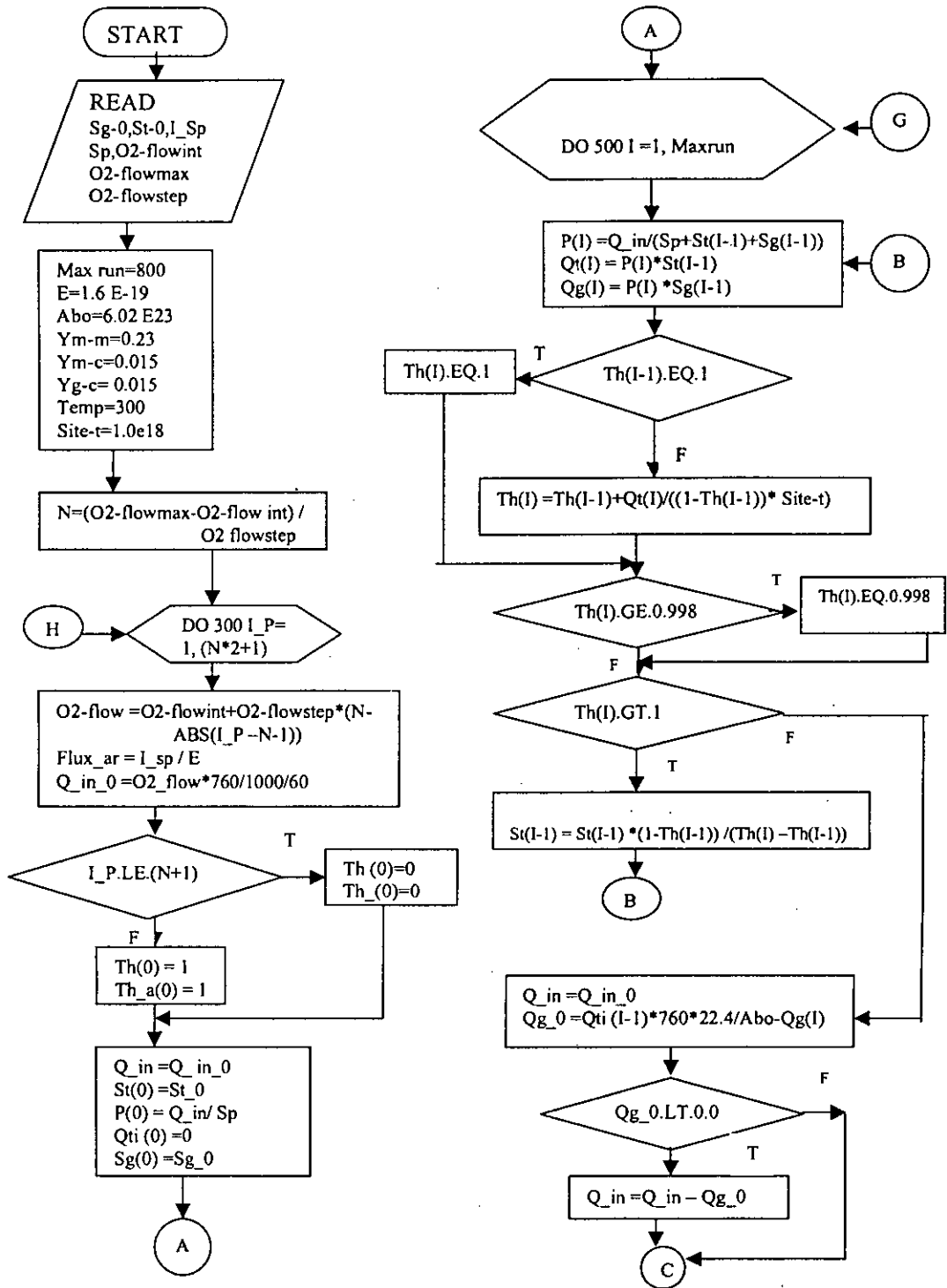
$$S_t(t) = (1 - \theta'(t)) S_t^0 \dots \dots \dots (3.2.2.8)$$

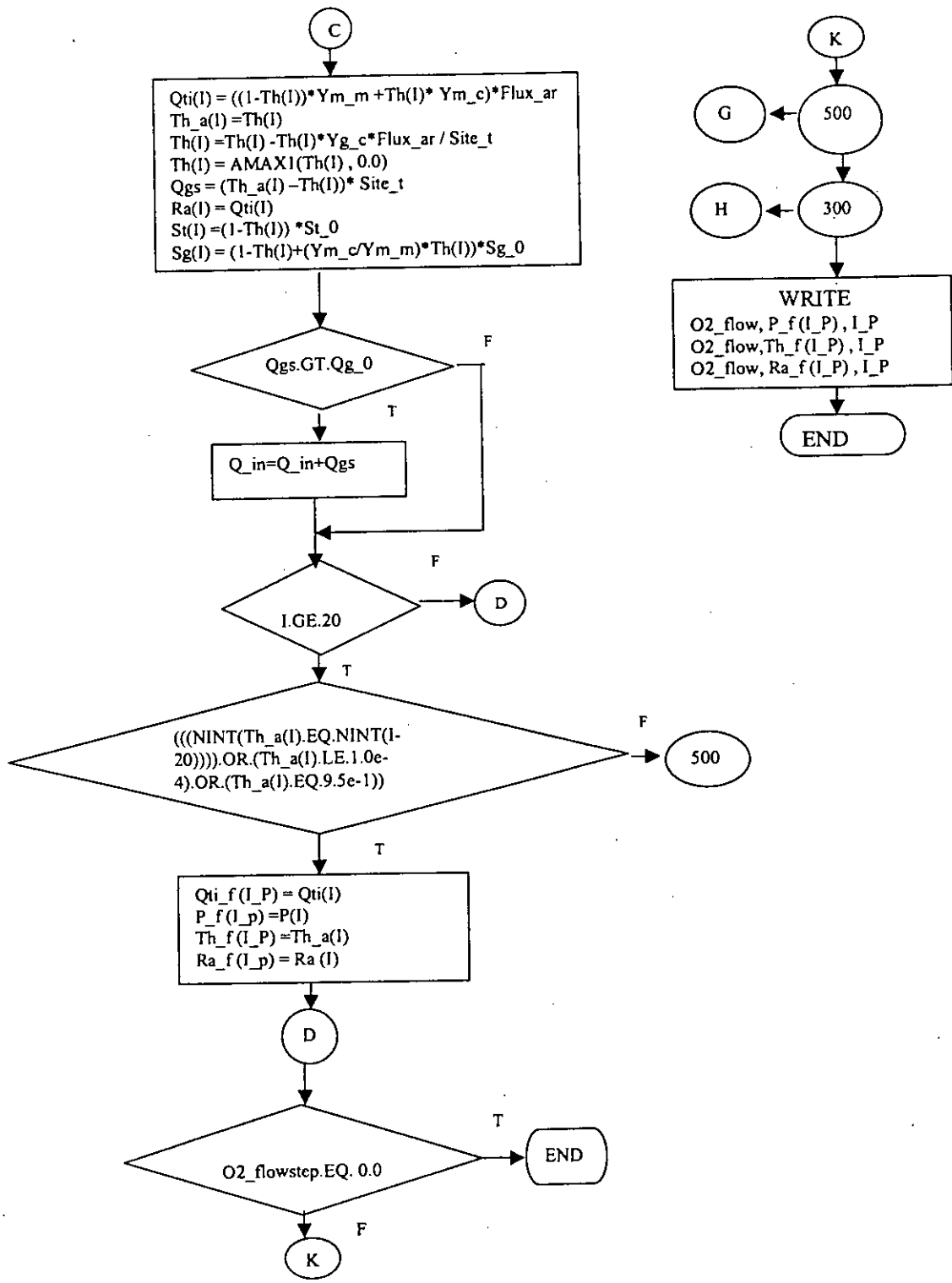
$$S_g(t) = (1 - \theta'(t) + Y_c / Y_m \theta'(t)) S_g^0 \dots \dots \dots (3.2.2.9)$$

After determining $S_t(t)$ and $S_g(t)$, the calculation of next time step, $T=t+1$, starts.

Hysteresis curves are obtained by calculating steady-state values of target compound-layer formation and sputter-etching for a range of Q_{in} . The calculation is started from $Q_{in} = 0$ std.cm³/min with the initial $\theta, \theta_i = 0$. Then, until the transition is observed, Q_{in} is increased in step of 0.5 std.cm³/min. After the transition is observed, it is decreased by the same step, starting the calculation with $\theta_i = 1$. In the hysteresis calculations, S_p and I_{sp} are varied.

3.2.3 Flow Chart





Chapter 4

DISCUSSIONS ON HYSTERESIS EFFECTS

4.1 Mass Balance Change During Compound Layer Formation and Sputter Etching

Target behavior in reactive sputtering is thought to be given as a consequence of two competitive phenomena: the formation of compound layers and the sputtering of formed compound layers; i.e., when the formation of compound layers overcomes the sputtering of formed compound layers, target is continuously covered with compound layers until two phenomena balances, and when the sputtering overcomes the formation, the target is continuously sputter-etched until two phenomena balances.

At a higher pumping speed, the compound-layer formation is suppressed since a larger amount of reactive gas is pumped out. On the other hand, at a lower pumping speed, the compound-layer formation is accelerated and reaches a steady state faster since a smaller amount of reactive gas introduced and sputtered from the target surface is pumped out in this condition. Sputtering current also influences compound-layer formation and sputter etching. At a higher current, the target is not covered with compound layers since sputter-etching overcomes compound formation, and sputtered metal getters more reactive gas, reducing the amount of reactive gas arriving target surface, thus target sputter- etching being accelerated.

The mechanisms of avalanche-like mode transition are explained as follows from the above discussion on the basic treatment in the model program;

1. When reactive gas flow rate exceeds slightly a critical point where wall gettering cannot consume enough reactive gas, surplus reactive gas is generated and reactive gas partial pressure is increasing.
2. this increase in reactive gas partial pressure further accelerates the formation of compound layers on the target surface
3. as compound layers cover target surface, metal atom flux generated by sputtering decreases, resulting in the decrease in wall gettering capacity, triggering an avalanche-like mode transition.
4. this correlation between the compound-layer formation on target surface and wall gettering capacity, triggering an avalanche-like mode transition.

4.2 Mechanisms of Hysteresis Formation

The hysteresis of sputter etching or total pressure in relation to reactive gas flow rate is a well-known behavior in reactive sputtering. This hysteresis is a consequence of the fact that the points where a change in the process condition occurs when the reactive gas flow rate is increased are different from the points where a change in the process condition occurs when the reactive gas flow rate is decreased.

The change in the process is drastic and avalanche-like, and is caused by the target surface condition change from a metallic condition to a compound-covered condition or from a compound-covered condition to a metallic condition, as a function of reactive gas flow rate. The target surface condition change is believed to correlate to gettering on the chamber wall. The resultant process is generally called mode transition: i.e., metal-compound (nonreactive-reactive) mode transition and compound-metal (reactive-nonreactive) mode transition.

The target surface condition change is a result of two competitive phenomena: formation of compound layers by chemisorption of reactive gas to active metal sites and sputtering of formed compound layers. This resulting change is affected by mass balance between the reactive gas and metal atoms or ions sputtered from target and by the arrival inert/reactive gas flux ratio. On the other hand, reactive gas gettering is considered to be a result of interaction between arrival reactive gas flux and sputtered metal flux to the chamber wall where gettering takes place. The interaction depends on reactive gas mass flow rate and the sputtering current that determines the sputtered metal flux. In addition to these factors, since gettering is thought to be in competition with evacuation of reactive gas by the vacuum pumping system, hysteresis is considered to be affected by physical pumping speed of the pumping system.

Mechanisms of hysteresis formation can be discussed by considering the role of getter pumping in the model. In the simulation program, since S_g is given as a function of θ , in the metallic condition (i.e., θ is very small), the total pumping speed of getter pumping and pumping of the vacuum pump is so large that the transition occurs at a higher reactive gas mass flow rate; on the other hand, in the compound-covered condition, since getter pumping speed is decreased as the target is covered with compound layers, the total pumping speed is lower than that in the metallic condition, resulting in that the inverse transition occurs at a lower reactive gas mass flow rate. Getter pumping dominates the mode transition from metallic to compound-covered condition since getter pumping speed is higher than pumping speed of vacuum pump affect the mode transition from compound-covered to metallic since S_g is decreased and becomes comparable to S_p as the target surface is covered with compound layers. Therefore, variation of S_p affects the transition from metallic to compound –covered condition to metallic, resulting in the decrease in the hysteresis width at higher S_p , whereas variation of I_{sp} affects the transition from metallic to compound –covered condition more, resulting in the increase in the hysteresis width at higher I_{sp} . For the various values obtained by simulation program, the hysteresis curves for sputtering rate, reactive gas partial pressure and coverage are drawn.

4.3 An Investigation of Hysteresis Effects as a Function of Pumping Speed and Sputtering Current

4.3.1 Effects of Pumping Speed

Figure 4.1 (a) shows the variation of the sputtering rate for increasing and decreasing the reactive gas flow for a pumping speed of 2 sccm. It is observed from the figure that the sputtering rate decreases with the increase of reactive gas flow rate. This is due to the compound layer formation on the target surface and from the reduced sputtering yield of the reactive gas molecules. The transition from metal to compound mode occurs at a oxygen flow rate of 5 sccm for increasing reactive gas flow and when the reactive gas flow rate decreases the reverse transition from compound to metal mode occurs at 4.5 sccm. Therefore, a clear hysteresis nature is observed. The hysteresis curves for sputtering rate for the pumping speeds of 0.3 m³/sec and 0.4 m³/sec are shown in 4.1(b) and 4.1(c) respectively. From these three curves it is found that transition points from metal to compound mode occurs at a higher oxygen flow rate and hysteresis width decreases with the increase of pumping speed. This is due to the fact that at higher pumping speed, a larger amount of oxygen is pumped out, so a larger amount of oxygen is required to obtain compound target. Again, when reactive gas flow decreases, the transition from compound occurs at higher oxygen flow rate for higher pumping speed, Sp. But, for lower pumping speed, reactive gas flow should be decreased more which causes larger hysteresis width at lower pumping speed.

Variation of reactive gas partial pressure with increasing and decreasing the reactive gas flow for the pumping speed of 0.2 m³/sec is shown in Fig. 4.2(a). This figure shows that the reactive gas partial pressure is low for metal mode where the target is not fully covered with compound layer. It is also observed that the reactive gas partial pressure increases with the increase of the reactive gas flow. This can be explained by partial formation of compound layer on the

gettered surface. The transition from metal to compound occurs at 5 sccm. However, after the target is fully covered with compound layer, the excess amount of reactive gas is present in the chamber causes higher reactive gas partial pressure. But, when reactive gas flow decreases, the reverse transition from compound to metal occurs at 4.5 sccm. The hysteresis curves for reactive gas partial pressure are drawn for pumping speeds of $0.3 \text{ m}^3/\text{sec}$ and $0.4 \text{ m}^3/\text{sec}$ and shown in Figs 4.2(b) and 4.2(c) respectively. It is found that transition points from metal to compound mode occurs at a higher reactive flow rate and hysteresis width decreases with the increase of pumping speed.

Figure 4.3 (a) shows the target coverage at a pumping speed of $0.2 \text{ m}^3/\text{sec}$ for the increase and decrease of the reactive gas flow. From this curve, it is observed that the coverage of compound layer at the target surface increases with the increase of reactive gas flow and transition from metal to compound mode occurs at 5 sccm. At compound mode, the coverage of compound reaches the steady state value of 1.0. When, reactive gas flow decreases the transition from compound to metal mode occurs at 4.5 sccm. The hysteresis curves for coverage for pumping speeds of $0.3 \text{ m}^3/\text{sec}$ and $0.4 \text{ m}^3/\text{sec}$ are shown in figs. 4.3(b) and 4.3(c) respectively. Here, also, it is found that transition points from metal to compound mode occurs at a higher reactive gas flow rate and hysteresis width decreases with the increase of pumping speed.

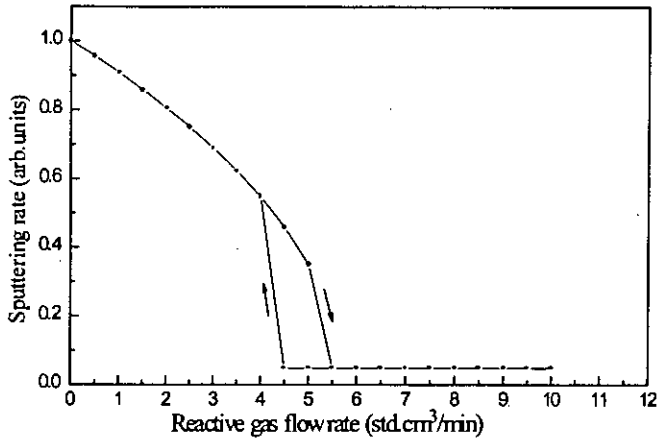


Fig 4.1(a) the variation of the sputtering rate for increasing and decreasing the reactive gas flow for a pumping speed of $0.2 \text{ m}^3/\text{sec}$

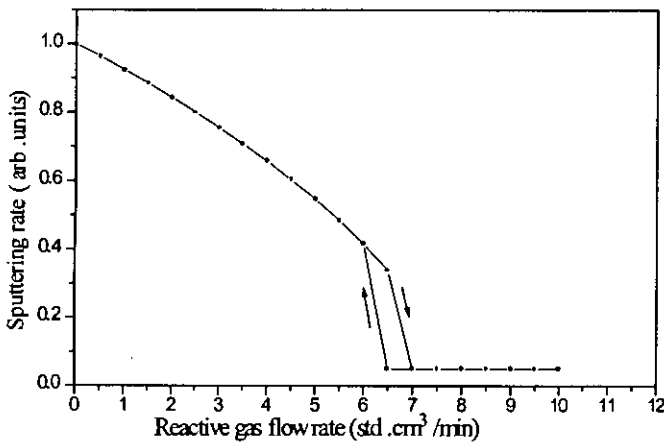


Fig 4.1(b) the variation of the sputtering rate for increasing and decreasing the reactive gas flow for a pumping speed of $0.3 \text{ m}^3/\text{sec}$

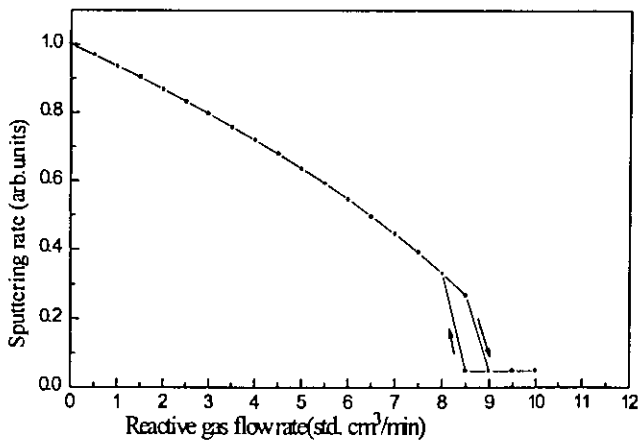


Fig 4.1(c) the variation of the sputtering rate for increasing and decreasing the reactive gas flow for a pumping speed of $0.4 \text{ m}^3/\text{sec}$

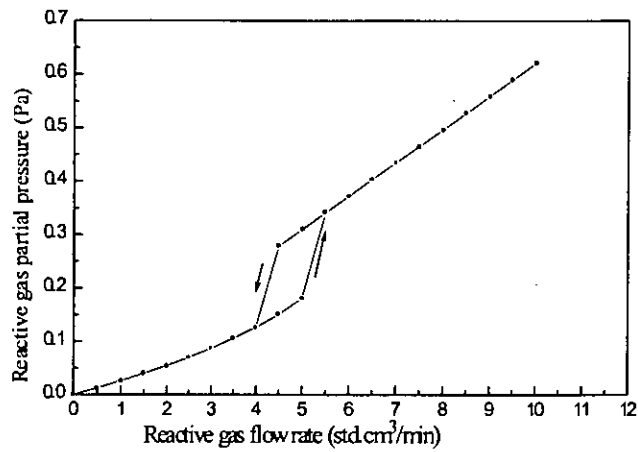


Fig 4.2(a) the variation of reactive gas partial pressure for increasing and decreasing the reactive gas flow for a pumping speed of $0.2 \text{ m}^3/\text{sec}$

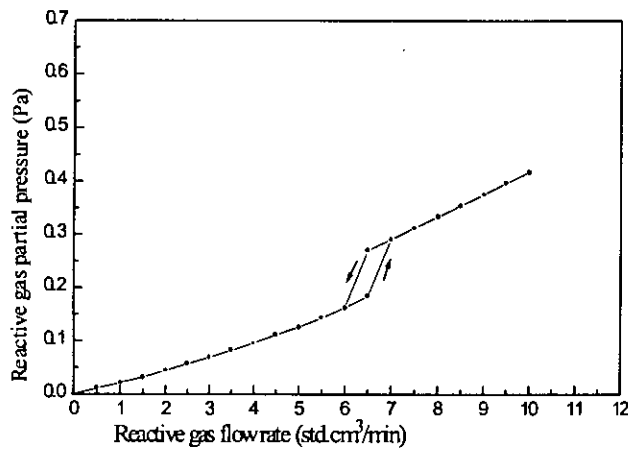


Fig 4.2(b) the variation of reactive gas partial pressure for increasing and decreasing the reactive gas flow for a pumping speed of $0.3 \text{ m}^3/\text{sec}$

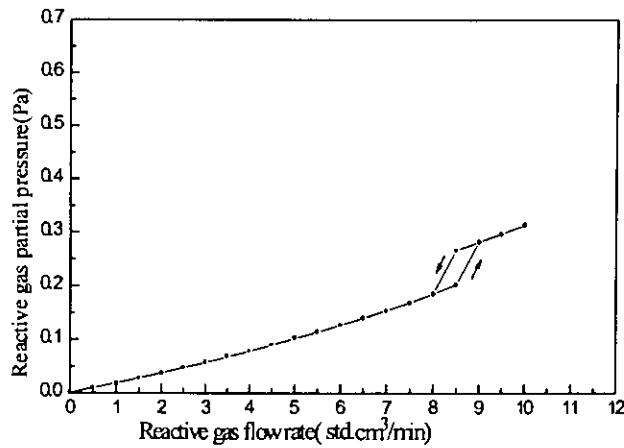


Fig 4.2(c) the variation of reactive gas partial pressure for increasing and decreasing the reactive gas flow for a pumping speed of $0.4 \text{ m}^3/\text{sec}$

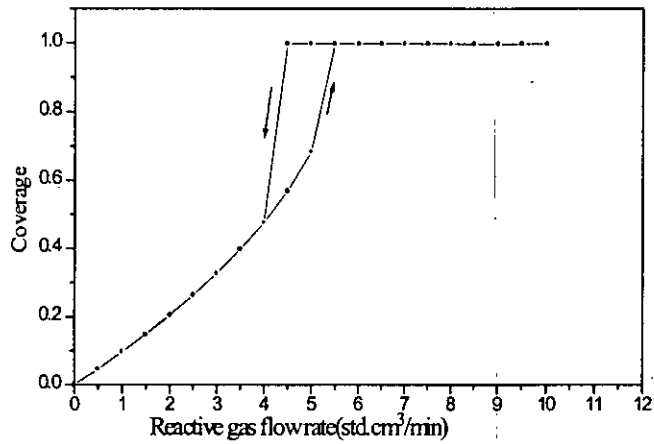


Fig 4.3(a) the variation of oxide layer coverage at the target surface for increasing and decreasing the reactive gas flow for a pumping speed of $0.2 \text{ m}^3/\text{sec}$

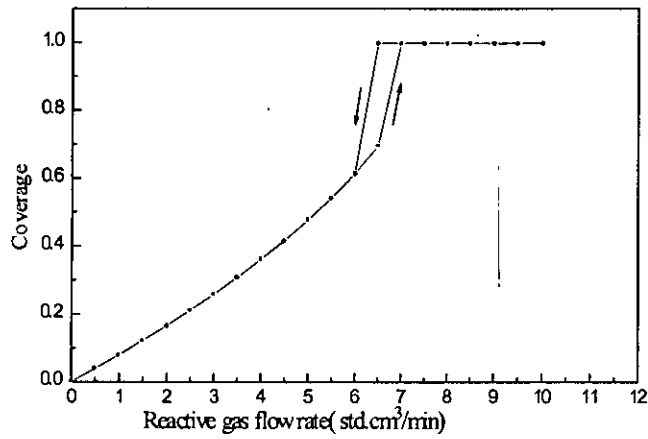


Fig 4.3(b) the variation of oxide layer coverage at the target surface for increasing and decreasing the reactive gas flow for a pumping speed of $0.3 \text{ m}^3/\text{sec}$

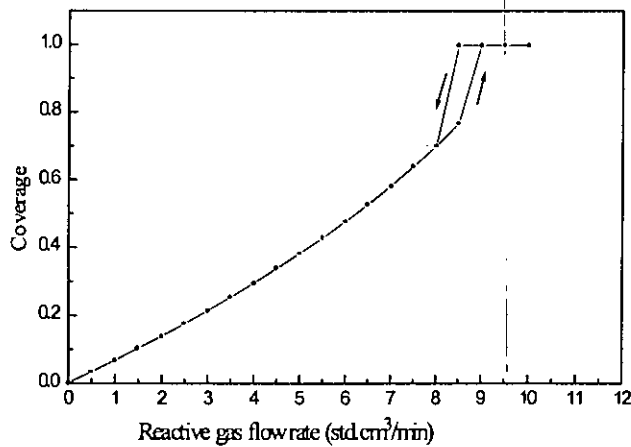


Fig 4.3(c) the variation of oxide layer coverage at the target surface for increasing and decreasing the reactive gas flow for a pumping speed of $0.4 \text{ m}^3/\text{sec}$

TABLE 1: Comparison Between Simulated and Experimental Results for Increasing and Decreasing Reactive Gas Flow Rate for Different Pumping Speed

| | Pumping Speed (m ³ /sec) | Simulated Results | | Experimental Results ²⁴ | |
|-----------------------------------|-------------------------------------|---|---|---|---|
| | | Transition point from Metal to compound mode due to Increase of Oxygen flow Rate (std.cm ³ /min) | Transition point from Compound to metal mode Due to Decrease of Oxygen flow Rate (std.cm ³ /min) | Transition point from Metal to compound mode due to Increase of Oxygen flow Rate (std.cm ³ /min) | Transition Point from Compound to metal mode Due to Decrease of Oxygen flow Rate (std.cm ³ /min) |
| Sputtering Rate (arb.units) | 0.2 | 5 | 6 | 4.5 | 5 |
| | 0.3 | 6.5 | 7 | 6.5 | 6.5 |
| | 0.4 | 8.5 | 8.5 | 8.25 | 8.25 |
| Reactive Gas partial Pressure(pa) | 0.2 | 5 | 6 | 4.5 | 5 |
| | 0.3 | 6.5 | 7 | 6.5 | 6.5 |
| | 0.4 | 8.5 | 8.5 | 8.25 | 8.25 |
| Coverage | 0.2 | 5 | 6 | 4.5 | 5 |
| | 0.3 | 6.5 | 7 | 6.5 | 6.5 |
| | 0.4 | 8.5 | 8.5 | 8.25 | 8.25 |

Table 1 shows that the theoretical results conformed with the experiment results.

4.3.2 Effects of Sputtering Current

In addition to the effects of S_p , the effects of sputtering current (I_{sp}) on hysteresis were investigated at $S_p = 0.3 \text{ m}^3/\text{sec}$ and $S_g = 0.3 \text{ m}^3/\text{sec}$. As before, the generic hysteresis curve for sputtering rate, reactive gas partial pressure and coverage are drawn for various sputtering current. Sputtering current influences compound layer formation and sputter etching. At a higher sputtering current, the target is not covered with compound layers easily since, sputter etching overcomes compound formation and sputtered metal getters most of the introduced reactive gas into the chamber, reducing the amount of reactive gas arriving at the target surface. So, the compound formation occurs at higher reactive gas flow rate. On the other hand, for higher I_{sp} , the depth of penetration of compound layer at target surface is greater than with lower I_{sp} . So, a larger amount of reactive gas should be reduced in the chamber for higher I_{sp} than with lower I_{sp} , causes the hysteresis width to increase at higher I_{sp} .

Figs. 4.4 (a), 4.4 (b) and 4.4 (c) are the generic hysteresis curves of sputtering rate. From this curve, it is found that transition point of metal to compound mode shifts from 2.5 sccm 7.5 sccm as the sputtering current increases from 1.0 amp to 3.0 amps. Figs. 4.5 (a), 4.5 (b), 4.5 (c) and figs. 4.6 (a), 4.6 (b), 4.6 (c) are the generic hysteresis curves of reactive gas partial pressure and coverage respectively. These figures also reveal that transition points of metal to compound mode shift to higher values of reactive gas flow rate with the increase of sputtering current.

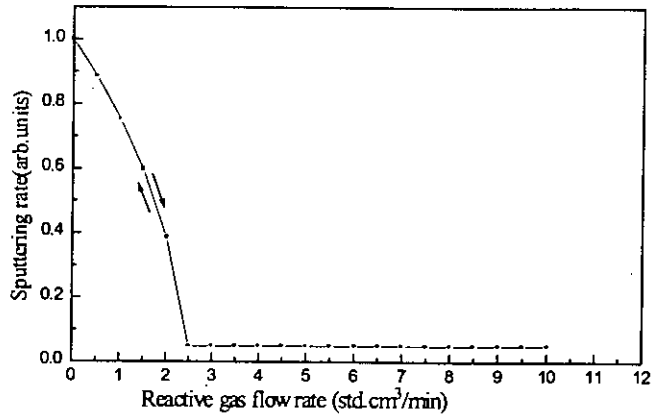


Fig 4.4(a) the variation of sputtering rate for increasing and decreasing the reactive gas flow for a sputtering current of 1 amp

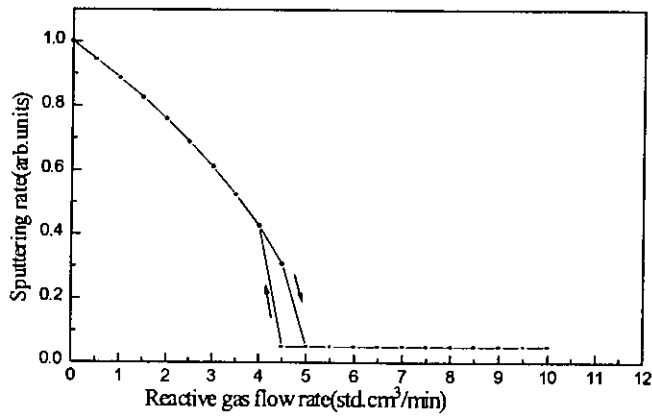


Fig 4.4 (b) the variation of sputtering rate for increasing and decreasing the reactive gas flow for a sputtering current of 2 amp

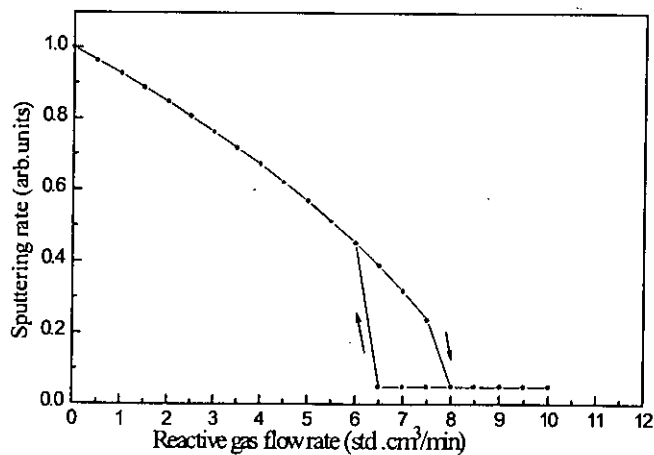


Fig 4.4 (c) the variation of sputtering rate for increasing and decreasing the reactive gas flow for a sputtering current of 3 amp

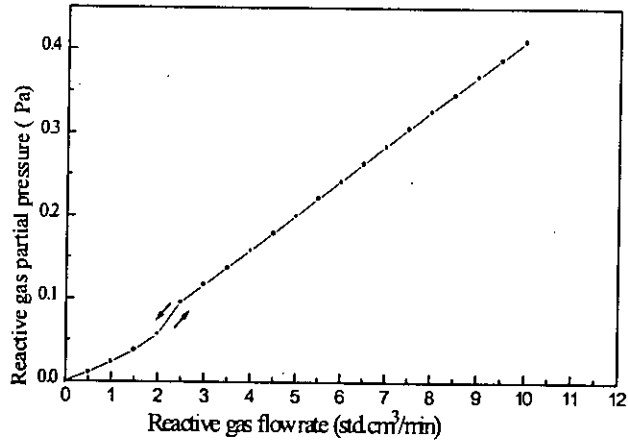


Fig 4.5(a) the variation of reactive gas partial partial pressure for increasing and decreasing the reactive gas flow for a sputtering current of 1 amp

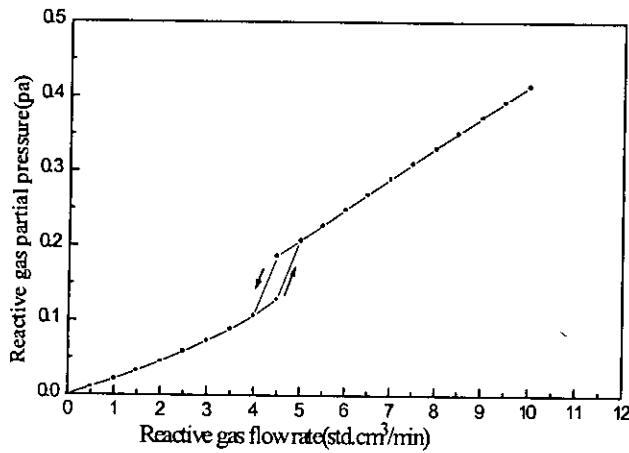


Fig 4.5(b) the variation of reactive gas partial partial pressure for increasing and decreasing the reactive gas flow for a sputtering current of 2 amp

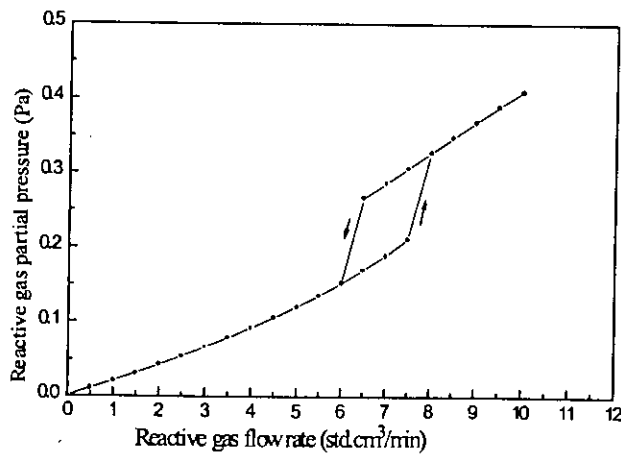


Fig 4.5(c) the variation of reactive gas partial partial pressure for increasing and decreasing the reactive gas flow for a sputtering current of 3 amp

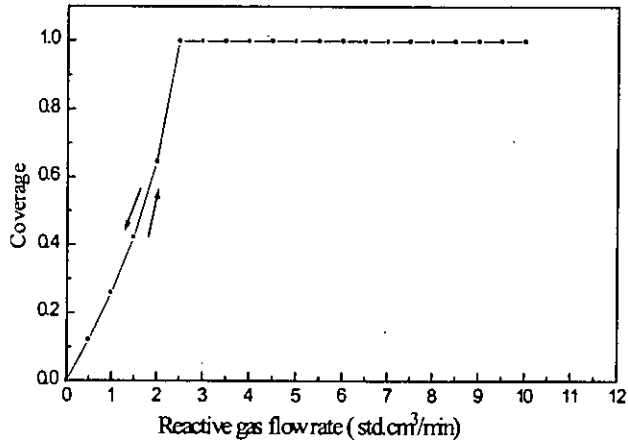


Fig 4.6(a) the variation of oxide layer coverage at the target surface for increasing and decreasing the reactive gas flow for a sputtering current of 1 amp

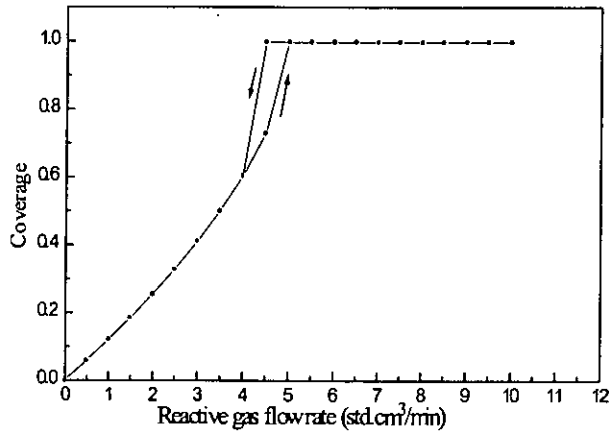


Fig 4.6(b) the variation of oxide layer coverage at the target surface for increasing and decreasing the reactive gas flow for a sputtering current of 2 amp

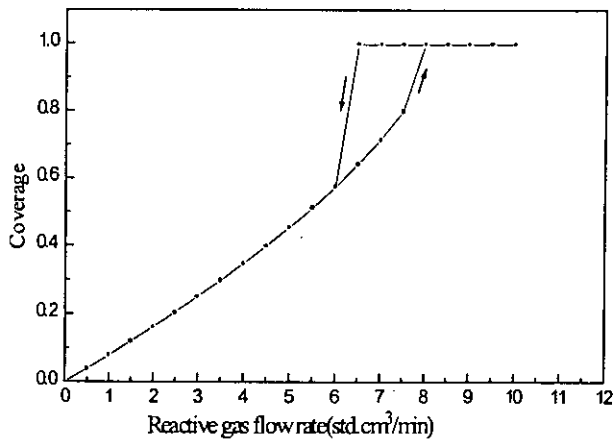


Fig 4.6(c) the variation of oxide layer coverage at the target surface for increasing and decreasing the reactive gas flow for a sputtering current of 3 amp

TABLE 2: Comparison Between Simulated and Experimental Results For Increasing and Decreasing Reactive Gas Flow Rate for Different Sputtering Current

| | Sputtering Current (Amp) | Simulated Results | | Experimental Results ²⁴ | |
|------------------------------------|--------------------------|---|---|---|---|
| | | Transition Point from Metal to Compound Mode Due to Increase of Oxygen Flow Rate (std.cm ³ /min) | Transition Point from Compound to Metal Mode Due to Decrease of Oxygen Flow Rate (std.cm ³ /min) | Transition Point from Metal to Compound Mode Due to Increase of Oxygen Flow Rate (std.cm ³ /min) | Transition Point from Compound to Metal Mode Due to Decrease of Oxygen Flow Rate (std.cm ³ /min) |
| Sputtering Rate (arb.units) | 1 | 2.5 | 2.5 | 2.5 | 2.5 |
| | 2 | 4.5 | 4.5 | 4.5 | 4.5 |
| | 3 | 7.5 | 6.5 | 7.5 | 6.5 |
| Reactive Gas Partial Pressure (Pa) | 1 | 5 | 6 | 4.5 | 5 |
| | 2 | 4.5 | 4.5 | 4.5 | 4.5 |
| | 3 | 7.5 | 6.5 | 7.5 | 6.5 |
| Coverage | 1 | 5 | 6 | 4.5 | 5 |
| | 2 | 6.5 | 7 | 6.5 | 6.5 |
| | 3 | 8.5 | 8.5 | 8.25 | 8.25 |

From the Table 2, it is observed that the simulated results are nearly equal to the experimental results

Chapter 5

CONCLUSIONS

5.1 Conclusions

The reactive sputtering process is a highly non-linear process. Due to ever increasing demand on film quality, the need for reliable processes offer an easy way of exploring possible new operating conditions.

A model simulating reactive sputtering mass balance changes has been proposed. The important feature of the model is that hysteresis curves are obtained as a result of the calculation of time-dependent target condition changes. This approach to obtain hysteresis curves is more similar to an actual reactive sputtering process.

This thesis presented a study of mechanisms involved in reactive sputtering process. Mass balance changes in reactive sputtering were strongly related with gettering behavior, and therefore related with pumping speed and with sputtering current.

Hysteresis curves are provided as a result of compound-layer formation and sputter-etching calculations. The effects of pumping speed and sputtering current on hysteresis curves are investigated. The investigation provided the following results:

- i. as pumping speed increases, the width of hysteresis decreases.
- ii. as sputtering current increases, the width of hysteresis increases.

The results obtained from the model calculation revealed mechanisms of hysteresis formation, i.e., the hysteresis is formed as a consequence of the

difference between the target surface. This difference was resulted from the difference in sputtering yields of a compound-covered target to that of a metallic target.

5.2 Recommendations for Further Work

In this thesis, a model simulating mode transition and hysteresis phenomena of single target using single reactive gas is presented. However, this model can also be extended to investigate multi target and multi reactive gas sputtering process.

Again, in this thesis, reactive sputtering process has been discussed considering reactive gas partial pressure in the chamber. However, the model will be more accurate by considering also the sputtering pressure.

The simulation model can also be extended to analyze film property, i.e., the percentage of metal component and reactive gas component at metal mode and compound mode.

References

- [1] B.Chapman, Glow Discharge Processes (John Wiley & Sons, New York, 1980), Chapter- 6, pp.177-184.
- [2] J.H. Grenier, "Josephson tunneling barriers by rf sputter etching in an oxygen plasma", J.Appl.Phys.42, 5151(1971).
- [3] J. Heller, "Reactive sputtering of metals in oxidizing atmospheres", Thin Solid Films 17, 1639(1973).
- [4] B. Goranchev, V. Ornov, and V. Popv, "D.C. cathode sputtering Influence of the oxygen content in the gas flow on the discharge current", Thin SoliFilms 33,173 (1976).
- [5] T. Abe and T. Yamashina, "Process modeling of reactive sputtering", Thin Solid Films 35, 19(1976).
- [6] L.F.Donaghey and K.G.Gerathy, "Effect of target oxidation on reactive sputtering rates of titanium in argon-oxygen plasmas", Thin Solid Films 38, 71(1976).
- [7] S. Maniv and W. D. Westood, "The current voltage characteristic of magnetron sputtering systems", J. Appl.Phys., 54(12), pp.6841-6846(1983).
- [8] R. McMahon, J. Affinito, and R.R. Parsons, "Voltage controlled, reactive planar magnetron sputtering of AlN thin films", J.Vac.Sci.Technol 20(3), 376(1982).
- [9] J. Affinito, and R.R. Parsons, "Mechanisms of voltage controlled, reactive, planar magnetron sputtering of Al in Ar/N₂ and Ar/O₂ atmospheres", J. Vac. Sci. Technol. A2(3), 1275(1984).
- [10] T.M. Reith and P.J. Ficalora, "The reactive sputtering of tantalum oxide: Compositional uniformity, phases, and transport mechanisms", J.Vac.Sci. Technol.A1(3), 1362(1983).
- [11] D.K. Hohnke, D.J. Scmatz, and M.D. Hurely, "Reactive sputter deposition: A quantitative analysis", Thin Solid Films 118, 301(1984).
- [12] T. Serikawa and A.Okamoto, "Effect of N₂-Ar mixing on the reactive sputtering characteristics of silicon", Thin Solid Films 101,1(1983).

- [13] A. Okamoto and T. Serikawa, "Reactive sputtering characteristics of silicon in an Ar-N₂ mixture", *Thin Solid Films* 137,143(1986).
- [14] Ch. Steinbruchel and D.M.Gruen , "Absolute measurement of sputtered ion fractions using matrix isolation spectroscopy", *Surf.Sci.*93, 299(1980).
- [15] D.M. Gruen , A.R. Krauss, and M.J. Pellin, "Effects of monolayer coverages on substrate sputtering yields", *Radiation Effects* 89, 113(1985).
- [16] G. Betz and W. Husinsky, *Nuclear Instruments and Methods in Physics Research B*13, 343(1986).
- [17] G. Lemperiere and J.M. Poitevin, "Influence of the nitrogen partial pressure on the properties of D.C - sputtered titanium and titanium nitride films", *Thin Solid Films* 111, 339(1984).
- [18] A.F. Hmiel, "Partial pressure control of reactively sputtered titanium nitride", *J.Vac.Sci.Technol.*A3(3), 592(1985).
- [19] S. Kadlec , J. Musil, and J. Vyskocil, IPAT 87, Proceedings of the 6th International Conference on Ion and Plasma Assisted Techniques, Brighton UK, pp. 184-189(1987).
- [20] S. Berg, H-O. Blom, T. Larsson, and C. Nender, "Predicting thin-film stoichiometry in reactive sputtering", *J.Vac.Sci.Technol.* A5(2), pp.887-891(1988).
- [21] S.Berg, H-O. Blom, C .Nender, M. Moradi, and C. Nender, "Process modeling of reactive sputtering", *J.Vac. Sci .Technol.* A7(3), pp.1225 - 1229(1989)
- [22] S. Berg, T. Larsson, C .Nender, and H-O. Blom, "Predicting thin -film stoichiometry in reactive sputtering", *J.Appl.Phys.*63(3), pp.887-891(1988).
- [23] S. Berg, M. Moradi, C. Nender, and H-O.Blom, "Physical model for eliminating instabilities in reactive sputtering", *J.Vac.Sci.Technol.*A6(3), pp.1832-1836 (1987).
- [24] Eiji Kusano,"Analysis of reactive sputtering deposition process of TiO₂ films". Ph.D thesis, University of Tokyo, Japan.1992.

- [25] I. Safi, "Recent aspects concerning DC reactive magnetron sputtering of thin films:a review", *Surface and Coating Technology* 127(2000), pp.203-219.
- [26] Satoshi Hamaguchi, Anita A. Mayo, Stephen M. Rossnagel, David E.Kotecki, KeithR. Milkove, Cindy Wang and Curtis.E .Farrell, "Numerical simulatin of Etching and Deposition Processes", *Japanese Journal of Applied physics*. Vol.36(1997), pp.4762-4768, Part 1, No.7B, July 1997.

Appendix

c This program calculates the hysteresis of the reactive sputtering by means of assumed pumping speeds, gettering speed and target sputtering speed.

```
DIMENSION Th(800), Th_a(800)
DIMENSION Qti(800),Qt(800), Qg(800), St(800),
+ Sg(800)
DIMENSION Tm(200),Th_f(200),Sg_f(200),St_f(200),
+ Qti_f(200)
real Th, Th_a,Ym_m , Ym_c, Yg_c
real P(800), St,Sp, Max_run,I_sp,Qti,
+ O2_flow_int,P_f(200), Qg,Qt, Ra(800),Ra_f(200)
real Sg, O2_flow_step,O2_flow
real Tm,Th_f,Sg_f,St_f,N_o_in,O2_flow_max ,
+ Qti_f,Q_in_0,Q_in
```

```
OPEN(150,FILE='QD.FOR')
OPEN(160,FILE='QC.FOR')
OPEN(170,FILE='QF.FOR')
```

```
Write (*,*) "Input Sputtering Current"
Read (*,*) I_sp
Write (*,*) "Sputtering current ", I_sp , " A"
```

```
Write (*,*) "Input pumping speed"
Read (*,*) Sp
Write (*,*) "Pumping speed ",Sp, " Liter/Sec"
```

```
Write (*,*) "Input target adsorption speed"
Read (*,*) St_0
Write (*,*) "target adsorption speed ",St_0, " Liter/Sec"
```

```
Write (*,*) "Input gettering speed"
Read (*,*) Sg_0
Write (*,*) "target adsorption speed ",Sg_0, " Liter/Sec"
```

```
Write (*,*) "Type init O2 flow rate in sccm"
Read (*,*) O2_flow_int
```

```
Write (*,*) "Init O2 flow rate in sccm ", O2_flow_int
```

```
Write (*,*) "Type maximum O2 flow rate in sccm"
```

```
Read (*,*) O2_flow_max
```

```
Write (*,*) "Maximum O2 flow rate in sccm ", O2_flow_max
```

```
Write (*,*) "Type step O2 flow rate in sccm"
```

```
Read (*,*) O2_flow_step
```

```
Write(*,*) "Type step of O2 flow rate in sccm ", O2_flow_step
```

```
Max_run=800
```

```
E=1.6E-19
```

```
kb=1.38E-23
```

```
Abo=6.02E23
```

```
Ym_m=0.32
```

```
Ym_c=0.015
```

```
Yg_c=0.015
```

```
Temp=300
```

```
Site_t=1.0e18
```

```
N_case=(O2_flow_max-O2_flow_int)/O2_flow_step
```

```
WRITE(*,*) N_case
```

```
c MAIN LOOP
```

```
Do 300 I_p=1, (N_case*2+1)
```

```
    O2_flow=O2_flow_step*(N_case-ABS(I_p-N_case-1))+O2_flow_int
```

```
c init variable
```

```
Q_in_0=O2_flow*760/1000/60
```

```
Flux_ar=I_sp/E
```

```
N_o_in=2*O2_flow*Abo/(22.4*1000*60)
```

```
If (I_p .LE. (N_case+1)) then
```

```
    Th(0)=0
```

```
    Th_a(0)=0
```

```
Else
```

```
Th(0)=1
Th_a(0)=1
```

```
end if
```

```
Q_in=Q_in_0
St(0)=St_0
P(0)=Q_in/Sp
Qti(0)=0
Sg(0)=sg_0
```

```
c END GOSUB INIT VARIABLE
```

```
100 Do 500 I=1,Max_run
```

```
110 P(I)=Q_in/(Sp+St(I-1)+Sg(I-1))
Qt(I)=P(I)*St(I-1)
Qg(I)=P(I)*Sg(I-1)
```

```
IF (Th(I-1) .EQ. 1) Then
    Th(I) =1
```

```
Else
```

```
Th(I)=Th(I-1)+Qt(I)*Abo/(760*22.4)/
+ ((1-Th(I-1))*Site_t)
```

```
End if
```

```
if (Th(I) .GE. 0.998) then
    Th(I) =.998
endif
```

```
120 If (Th(I) .GT. 1) then
```

```
121
```

```
Qt_a=(1-Th(I-1))*Site_t
Qt_a=Qt_a*760*22.4/Abo
St(I-1)= St(I-1)*(1-Th(I-1))/(Th(I)-Th(I-1))
```

```

        goto 110
    end if

    Q_in=Q_in_0
    Qg_o=Qti(I-1)*(760*22.4)/Abo-Qg(I)

    If(Qg_o .LT. 0.0) then
        Q_in=Q_in-Qg_o
    End if

```

```

Qti(I)=((1-Th(I))*Ym_m+Th(I)*Ym_c)*Flux_ar
Th_a(I)=Th(I)
Th(I)=Th(I)-Th(I)*Yg_c*Flux_ar/Site_t
Th(I)=AMAX1(Th(I),0.0)
Qgs=(Th_a(I)-Th(I))*Site_t*(760*22.4)/Abo
Ra(I)=Qti(I)

```

C DET SPEED

```

St(I)=(1-Th(I))*St_0
Sg(I)=(1-Th(I)+(Ym_c/Ym_m)*Th(I))*Sg_0

```

```

write (*,*)I_p, I, Th(I),Th(I-1),Ra(I)

```

```

If (I .GE. 20) then
    If(((NINT(Th_a(I)) .EQ. NINT(Th_a(I-20)))) .OR.
+      (Th_a(I) .LE. 1.0e-4) .OR.
+ (Th_a(I) .EQ. 9.5e-1)) then

```

```

    Qti_f(I_p)=Qti(I)
    Tm(I_p)=I
    P_f(I_p)=P(I)
    Th_f(I_p)=Th_a(I)
    Ra_f(I_p)=Ra(I)
    St_f(I_p)=St(I)
    Sg_f(I_p)=Sg(I)

```

```

    If(O2_flow_step .EQ. 0) then
        goto 400
    end if
goto 500

```

```

        end if
    end if

500 end do

300 end do

Do 600 I3=1, (N_case*2+1)
    O2_flow=O2_flow_step*(N_case-ABS(I3-N_case-1))+O2_flow_int

    IF(I3.EQ.1)THEN
        TT= Ra_f(I3)
    ENDIF

    Write(150,*) O2_flow,P_f(I3),I3
    Write(170,*) O2_flow,Th_f(I3),I3
    Write(160,*) O2_flow,Ra_f(I3)/TT,I3
600 continue

400 END

```

